COMPARISON OF THE LONG BONE MICROSTRUCTURE OF TWO SOUTHERN AFRICAN MARINE BIRDS, THE CAPE GANNET (*Morus capensis*) AND THE AFRICAN PENGUIN (*Spheniscus demersus*) WITH RESPECT TO THEIR AQUATIC ADAPTATIONS

Vidushi Prema Dabee

Student number: DBXVID001

Submitted in the partial fulfillment of the requirements for

the degree of Bachelor in Science (Honours) in the

Department of Biological Sciences, Faculty of Science,

UNIVERSITY OF CAPE TOWN

September 2013

Supervisors: - Prof. Anusuya Chinsamy-Turan
Head, Biological Sciences
University of Cape Town
Private Bag X3
Rhodes Gift
7701 Rondebosch
Cape Town
South Africa

- Dr. Aurore Canoville
Postdoctoral Researcher
Palaeobiology Research Group
Dept. of Biological Sciences
University of Cape Town
Private Bag X3
Rhodes Gift
7701 South Africa

ABSTRACT

The Cape gannet (*Morus capensis*) and the African penguin (*Spheniscus demersus*) have distinct aquatic adaptations for locomotion. The gannet, which is an efficient flying bird, uses both fore- and hind limbs to propel itself under water. On the other hand, the flightless penguin swims underwater using only its forelimbs. In this study, the long bones of ten penguins and nine gannets were compared in terms of microanatomy and histology with respect to ontogenetic stage (hatchlings, juveniles and adults) and locomotion.

Micronatomical and histological findings of the fore-limbs and hind limbs show that the bone microstructure of the gannets and the penguins differs significantly in term of compactness and bone remodeling. Penguin bones are more thick-walled and compact as compared to gannet bones and their cortical tissue is dominated by simple vascular canals whilst the medullary cavity is nearly absent. The forelimb bones of penguins are more compact that the hind limb bones. This is due to the aquatic adaptation of the bone to fore-limb underwater propulsion. On the other hand, the gannet bones are thin walled, less compact with primary osteons dominating the mid-cortex, and a large vacant medullary cavity is present. The gannet fore- and hind limb bones do not differ in terms of bone compactness.

Ontogenetic differences in the penguin long bones show that the hatchling bears an active growth phase. Some of the bones of the juvenile penguins are still actively growing whilst the adult ones appear to have stopped growing as the bone mid-cortex is more organized. For the gannet species, the juvenile and adult differs in terms of the presence and thickness of the inner and outer circumferential layers and the presence of circumferential vascularizations.

Intra-specific differences are noted in the juvenile penguins with one specimen still undergoing active growth depicted by the presence of numerous simple vascular canals. Amongst the adult penguins, one male specimen is actively molting as indicated by the presence of large resorption cavities in all of the long bones. One adult gannet individual possesses large resorption cavities in all its long bones as a result of starvation caused by perforation of its intestines.

Inter-skeletal differences are noted with the stylopod and zeugopod being the most affected by sub-aquatic locomotion with osteosclerosis occuring the most in the proximal bone and decreases

in the distal bones going from the pectoral to the pelvic bones in the African penguin. In the Cape gannet, the stylopod and ulna have micro-structural features for torsional resistance during flight.

TABLE OF CONTENT

ACKNOWLEDGMENTS

I would like to express my sincere gratitude to the following people who helped me in achieving this report.

I am thankful to Dr. Aurore Canoville, my supervisor on this project. She taught me everything on bone microanatomy and histology, a topic that I had no previous knowledge of. Thank you for the incredible encouragement, patience and support; for all the help and contribution, comments and for making sure that my writing was intelligible.

My thanks to Prof. Anusuya Chinsamy-Turan, who introduced me to this project report. Her supervision provided me with all the insightful comments and perspectives to improve this project.

Besides my supervisors, I would like to thank by Dr. Nola Parsons (SANCCOB's veterinarian and researcher), who together with Dr. Aurore Canoville, acquired the biological sample in this project and therefore, made this project possible.

My deepest appreciation to Granville Faulmann, Andrea Plos, George Du Plessis and especially to Emil Krupandan, for their skillful technical support during the dark ages of broken machines. To Liesl Phigeland, Zama Jikumlambo and Soraya Abrabrams, for providing me with the necessary laboratory containers during the preparation of the bones for sectioning.

And extended thanks to Dr. Ragna Redelstorff, Germán Montoya Sanhueza and Dr. Ignacio Alejandro Cerda, who helped me to understand some concepts in this project. To Germán, for allowing me to use his camera, with which those magnificient pictures in this project were taken.

Special thanks to my family for their support, especially my father, Dr. Satiss Kumar Dabee for encouraging me to pursue further studies.

I wish to thank my boyfriend, Grant Leslie Barry Petersen for his loving encouragement and support, especially during this stressful time of final write-up.

My final thanks go to Miss Sandy Smuts who believed in my capabilities and gave me a chance to prove myself at honours level. I will be indefinitely grateful to her for giving my future a direction.

LIST OF TABLES

LIST OF FIGURES

INTRODUCTION

Throughout their evolution, birds have adapted their morphological structures and behavioural patterns with respect to their environment (flying, terrestrial, freshwater or marine) and foraging behaviour (Kato et al, 2006; Habib and Ruff, 2008). Birds like the Frigate birds (*Fregata* species) are surface predators and they are pelagic piscivores that obtain their food on the wing. They do not swim under water and their adaptation to flight is efficient during their feeding pattern above the ocean surface (Vickery and Brooke, 1994). Some bird species such as the gannets (*Morus capensis*) or the cormorants (*Phalacrocorax capensis*) exhibit both aerial and sub-aquatic adaptations, i.e. they have bimodal locomotion (Ropert-Coudert, 2004). Lineages like the Spheniscidae have evolved such that flying skills have been lost to give way to excellent swimming and diving aptitudes. Birds that have developed sub-aquatic locomotion have also adapted various swimming and diving patterns that are energy-efficient and conserving (Kato et al, 2006). Birds, such as the cormorant (*Phalacrocorax* species) are hindlimb-propelled divers which use their hindlimbs for swimming. Spheniscidae are forelimb-propelled divers. Birds like the gannets have an intermediate adaptation for underwater diving by means of fore-limbs and hindlimbs propulsion (Ropert-Coudert, 2004).

Most avian cortical bone bears a primary bone structure which persists throughout the bird's life. Bird cortical bone is generally made up of highly oblique vascularized fibrolamellar bone consisting of primary osteons (de Ricqlès et al, 1991). In addition, a mixture of longitudinal, circumferential and radial primary osteons is also present in avian bone (de Ricqlès et al, 1991; de Margerie, 2002). However, the composition of the bone microstructure is greatly affected by habitat and locomotion (Habib and Ruff, 2008). Birds adapted primarily to flight possess a slender bone compacta as compared to their terrestrial counterparts (Dumont, 2010). Flightless birds adapted solely to an aquatic environment exhibit very compact bone whilst those of birds with bimodal locomotion lies somewhere in-between (Habib and Ruff, 2008).

Various studies have revealed that the limb bone microanatomy is important in understanding lifestyle adaptations of birds. For example, bone compactness is an important factor that allowed birds to adapt to an aquatic environment. Previous studies of marine adaptations of

tetrapod bone microanatomy examined involved only one adult specimen per species and only one or two limbs bones were used for comparisons (Wall, 1983; Fish and Stein, 1991; Kriloff et al, 2008). Furthermore, evaluations between fore-limbs and hind limbs during various ontogenetic stages were not examined. In addition, non-ecological adaptation factors have been found to transform bone histology and microanatomy (Starck and Chinsamy, 2002). Also, it has been shown that both intrinsic and extrinsic factors can influence bone microstructure (Chinsamy and Abdala, 2008).

The aims of this study is to assess how long bone microstructure and compactness changes during ontogeny in two marine taxa (*Morus capensis* and *Spheniscus demersus*) and to also document differences between genders and to the particular type of locomotion. Inter-skeletal variability between fore- and hind limbs will also permit an assessment of how specialized sub-aquatic locomotary adaptations affect bone microanatomy and histology. Comparisons will be made between the two marine bird taxa (*Morus capensis* and *Spheniscus demersus*) which exhibit different lifestyle adaptation to assess the effect of their specialized locomotary adaptations on their bones.

The main objectives of this study are:

- To assess the limb bone microstructure and compactness variability during ontogenesis of marine birds

-To study how the mode of locomotion affects the bone microanatomy

- To study the inter-specific variability between marine birds.

-To evaluate the intra-specific bone histological variability between individuals of the same age

- To determine intra-skeletal variability of the various long bones and which bones are most affected by sub-aquatic locomotion

-To determine physiological variables responsible for bone microanatomical differences

MATERIAL AND METHODS

In the present study, we employed histo-morphometry to quantify the cortical thickness of the bones, as well as qualitative descriptions of bone microanatomy and histology to assess inter- and intra- specific variability in the bone microstructure of two marine birds, *Morus capensis* and *Spheniscus demersus*.

Biological sample

A total of 19 individuals spread across two species of marine birds, with similar body size/body weight range, but with different aquatic adaptations, were included in the study sample. The African penguin species is represented by 10 individuals. Three developmental stages are included in this penguin study sample, namely, hatchling, juvenile and adult in ratio 1:3:6 (Table 1). Four juveniles and five adults of gannets are in the sample (Table 1).

The first species is the flightless *Spheniscus demersus* (Linnaeus, 1758), commonly known as the African penguin or Jackass penguin and is part of the penguin family Spheniscidae. These penguins can reach a height of 60–70 cm and weigh between 2.2–3.5 kg (Sinclair et al, 2011), and they exhibit some sexual dimorphism with males being larger and having heavier beaks than females. The African penguin exhibits a highly active sub-aquatic mode of locomotion using forelimb propulsion. They forage 33-46 km from their colonies and can dive to a mean depth of 17 m for 2.5 minutes (Wilson and Wilson, 1995). The species breeds monogamously all year round once they reach sexual maturity at the age of 3-7 years old with females maturing faster than males (Whittington et al, 2005). One to two eggs are laid and incubation lasts ~40 days and parents brood chicks for 15-30 days. Fledging occurs between 60-130 days after hatchling. Juveniles leave the colonies for 1 to 3 years (Kemper and Roux, 2005). African penguins return to their nest sites during annual molt (Cooper 1978). Juveniles undergo a pre-molt fattening-up phase (~34 days) followed by molting which takes about 21 days. Plumage replacement takes place after molting (~41 days) prior to the start of breeding (Randall and Randall, 1981). The overall duration of the molting phase is about 96 days per year. Juvenile penguins lose half their body mass during this period (Randall and Randall, 1981).

The second species consists of *Morus capensis* (Lichtenstein, 1823), commonly known as the Cape gannet belongs to the family Sulidae. It can reach a length of 84–94 cm from head to tail

and a mean body mass of 2.8 kg (Nelson, 1978). Males are larger than females, and females have a wider weight variation than males (Rand 1959). This species expresses efficient bimodal locomotion to fly or swim when foraging (Ashmole 1971). They use either their forelimb or hind-leg as a way of propelling themselves underwater. They are known to forage away from their colonies distances of 67-228 km and can plunge-dive from a height of 5-20 m to a mean depth of 3.6 m lasting 4.3 seconds (Grémillet et al, 2004; Ropert-Coudert et al, 2004). The Cape gannet breeds monogamously in late August on islands (Rand, 1959). One single egg is laid and the incubation lasts 42-46 days. Hatchlings remain in the nest for 93-105 days until the juveniles are fully fledged and leave the colonies. They have a fat storage of 10 days during which time they learn to forage. Molting into adult plumage occurs in juveniles at 4 years of age upon their return to the nesting sites prior to first breeding attempts (Jarvis, 1972). Adults molt in summer.

All osteological samples were obtained post-mortem from birds that died after unsuccessful rehabilitation at the Southern African Foundation for the Conservation of Coastal Birds (SANCCOB). Each bird was assigned a specimen number (Table 1). Data such as age, sex, cause of death, weight, size and area of collection were tabulated in Table A1 (Appendix section).

Bones of the left forelimb (humerus,radius, ulna and carpometacarpus) and hind limb (femur, tibiotarsus, tarsometatarsus and proximal phalanx) were sampled (Figure 1). These bones were selected since they are the skeletal elements most micro-structurally affected by locomotion and habitat (Habib and Ruff, 2008) and they also permit comparisons with previous histological papers. Some bones were not systematically sampled, such as the phalanges due to the extensive damage these bones were subjected to (Cause of death – Table A1). A few bones were missing in our sample, including the carpometacarpus and the femur of some specimens, because they were broken (Cause of death –Table A1). A total number of 136 bones were analyzed during this study. The whole bone sample is depicted in Figures A1- A4. The fore-limb and hind limb are divided into 3 distinct region during limb development (Shubin et al, 1997) : the stylopod (humerus/femur); the zeugopod (radius, ulna, tibiotarsus) and the autopod (carpometacarpus, tarsometatarsus and phalanx) (Figure 2).

Table 1: Data relevant to the biological samples showing the bird number assigned to each specimen, the species, age and gender. A completed data table is tabulated in Table A1. Picture of the African penguin species showing two adult, one juvenile in a lying position and an individual molting on the far right side. Cape gannet image showing adults (golden-white birds) and juveniles (black birds). Images courtesy of Dr. Aurore Canoville.

African penguin – *Spheniscus demersus*

Cape gannet – *Morus capensis*

N°	Bird N°	Species	Age	Gender
1	064	African penguin	Hatchling	Male
2	466	African penguin	juvenile	Female
3	116	African penguin	juvenile	Male
4	241	African penguin	juvenile	Male
5	146	African penguin	Adult	Male
6	191	African penguin	Adult	Male
7	192	African penguin	Adult	Male
8	167	African penguin	Adult	Female
9	231	African penguin	Adult	Female
10	524	African penguin	Adult	Female

N°	Bird N°	Species	Age	Gender
1	G04	Cape Gannet	juvenile	Male
2	G17	Cape Gannet	juvenile	Female
3	G19	Cape Gannet	juvenile	Male
4	G20	Cape Gannet	juvenile	Female
5	G59	Cape Gannet	Adult	Male
6	G61	Cape Gannet	Adult	Male
7	G24	Cape Gannet	Adult	Female
8	G56	Cape Gannet	Adult	Female
9	G57	Cape Gannet	Adult	Female

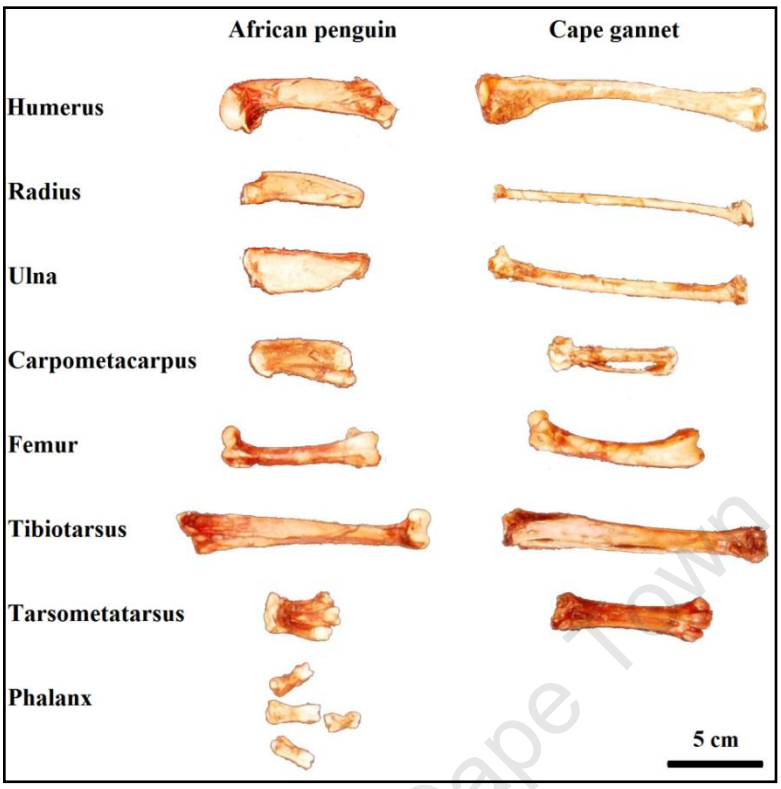

Figure 1: Representative example of African penguin (*Spheniscus demersus*) and Cape gannet (*Morus capensis*) long bones analyzed in this study. The fore limb bones are the humerus, radius, ulna and carpometacarpus. The hind limb bones are the femur, tibiotarsus, tarsometatarsus and phalanx. The bones are presented with their proximal ends on the left.

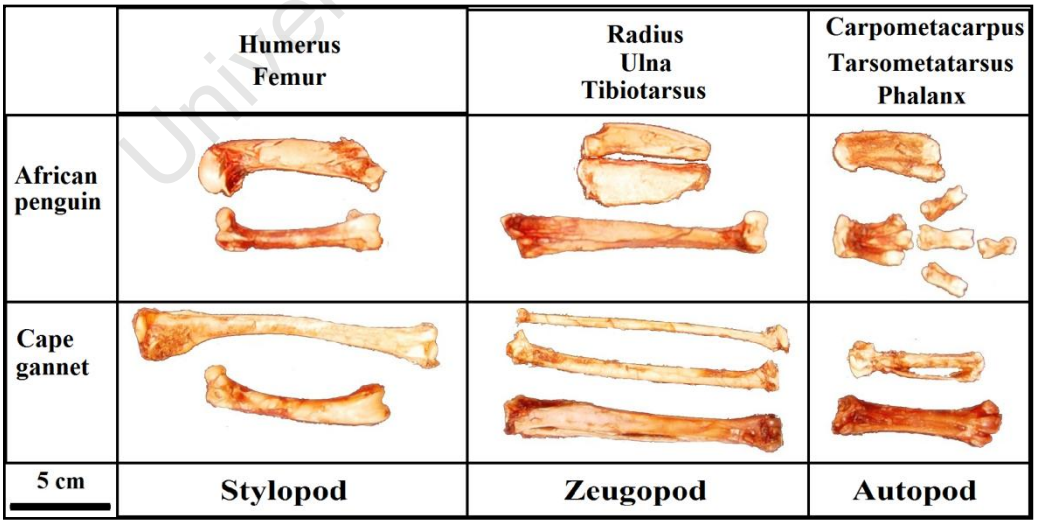

Figure 2: Classification of fore-limb and hind limb bones of the African penguin and the Cape gannet into stylopod, zeugopod and autopod with the proximal side on the left.

Bone preparation and sectioning

Carcasses of the birds were dissected in the Department of Biological Sciences, UCT in order to remove the bones for the study. As much flesh as possible was removed from the skeletal elements during dissection, and thereafter they were further subjected to treatment using mealworms and beetles. Pictures of the bone sample were taken using a Nikon D40 camera and were enhanced using PhotoScape image editor (PhotoScape software v3.6.3).

Standardized measurements of the bones were obtained with a digital caliper prior to sectioning and the mid-shaft level identified (Figure 3). Measurements include the bone maximal length, proximal width, distal width and mid-shaft diameter (Figure 3). All measurements were recorded in Tables A2-A3.

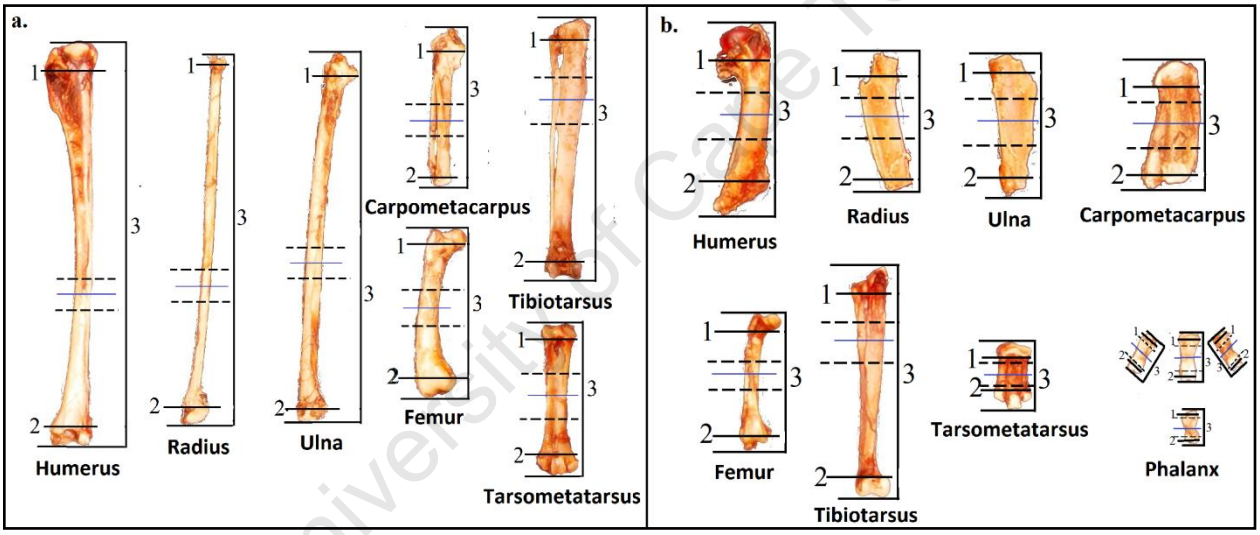

Figure 3: a. Cape Gannet (*Morus capensis*) bones. b. African Penguin (*Spheniscus demersus*) bones. Approximate positions at which measurements have been taken and cutting point for the mid-shaft region for each type of bones. The data is reported in Appendix, Tables A2-A3. [1: Proximal width; 2: Distal width; 3: Bone length; Blue line: Mid-shaft diameter; dotted black line: Cutting points]. [Bone sizes are not to scale].

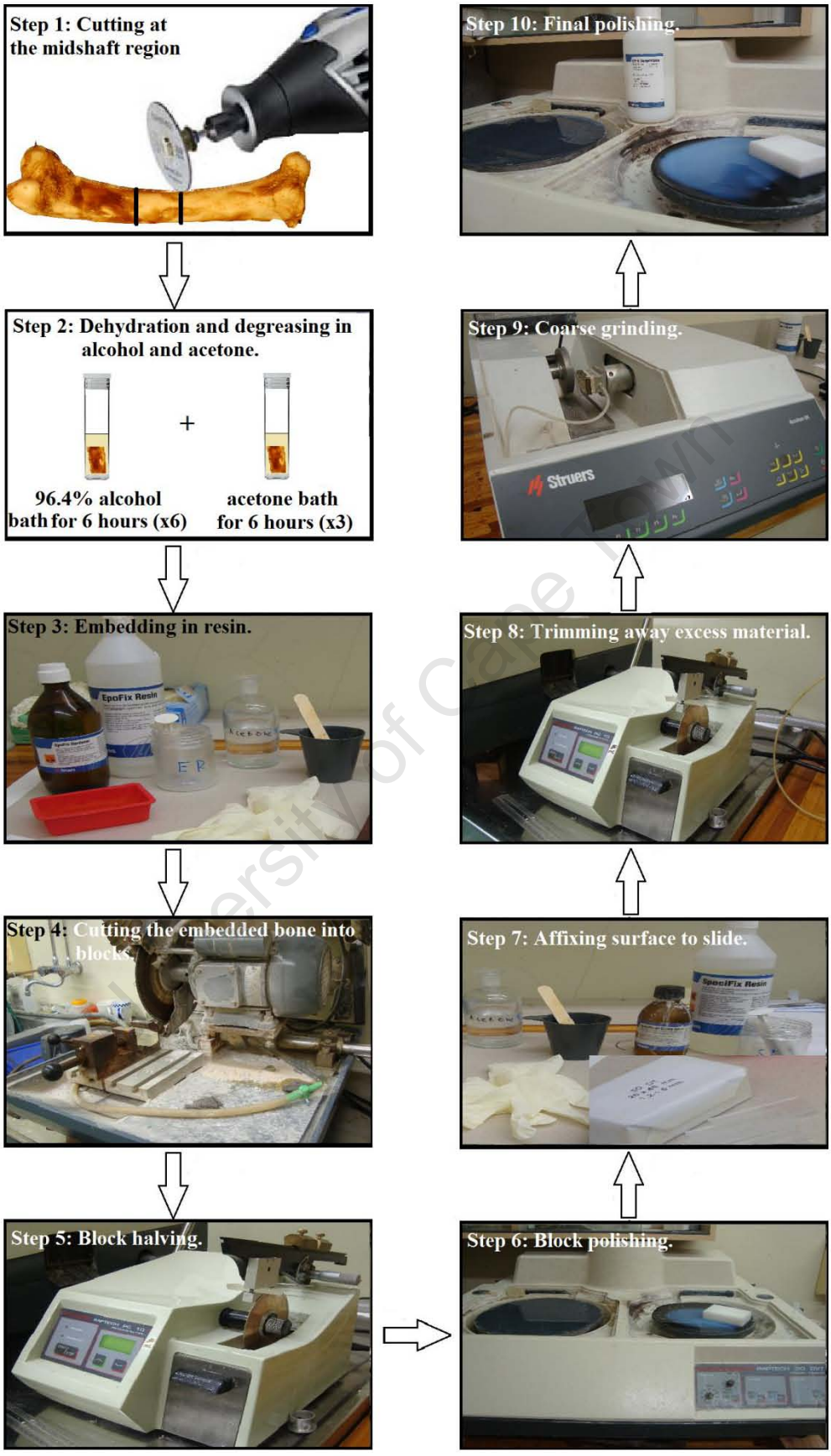
Step 1: Cutting at the midshaft region
Step 2: Dehydration and degreasing in alcohol and acetone.
+
96.4% alcohol bath for 6 hours (x6)
acetone bath for 6 hours (x3)
Step 3: Embedding in resin.
EpoFix Resin
Step 4: Cutting the embedded bone into blocks.
Step 5: Block halving.
Step 6: Block polishing.
Step 7: Affixing surface to slide.
SpeciFix Resin
Step 8: Trimming away excess material.
Step 9: Coarse grinding.
Struers
Step 10: Final polishing.

Figure 4: Steps in preparing bones for thin-sectioning following standard protocols detailed below.

The bones were then cut about 1-2 centimeter using a Dremel precision handsaw along the mid-shaft region (Figure 3) and more than 130 thin-sections were prepared following standard protocols (Chinsamy and Raath, 1992) (Step 1). The steps are illustrated in Figure 4. Each bone sample was subjected to six 96.4% ethanol baths and 3 acetone baths under a vacuum fume hood; each lasting 6 hours, in order to dehydrate and degrease the bones (Step 2). The bones were allowed to air dry for 24 hours prior to resin embedding. The bones were embedded in Struers Epofix Resin and Epofix Hardener with a volume mixture of 25:3 and left to harden for approximately 24 hours (Step 3). Using Imptech C10-abrasive cutter, the embedded bones were finely sectioned into blocks (Step 4), which were in turn halved along the mid-shaft line using a Struers Diamond cut-off wheel mounted on an Imptech PC10-precision cutter at a cutting speed of 150 rpm (Step 5). Half of the cut blocks were then sequentially polished using P800 and P1200 grit abrasive paper on an Imptech 30 DVT Grinder polisher machine (Step 6). Polishing was finalized using Struers OP-U silica suspension on a felt-polishing pad. The embedded bones were washed and left to dry for 24 hours on paper towels. Glass microscope slides of about 1.2-1.5 mm thick; having a frosted finishing side obtained by abrasion using silicon carbide powder; were used to mount the blocks. A fine spread of Struers Specifix Resin mixed with Specifix-20 Curing Agent (13:2.5 volume ratio) was applied to the polished side of the blocks and then affixed onto the frosted side of the slides (Step 7). All slides were properly labeled and fixing was allowed to set for 12 hours at room temperature. The next step involves cutting the excess embedded bone so as to leave ~2100 μm mid-shaft thickness with a Struers diamond-encrusted blade mounted in a Struers Accutom-50 machine (Step 8). The slides were further grounded using the Fine Grind option and the Struers diamond-encrusted grinding wheel to remove ~700 μm thickness or until the desired thickness is obtained for proper comparative microanatomy (Step 9). To ensure that the relevant thickness was attained, a Leica Galen III microscope was used intermittently during the grinding process. For the final step, the slides were polished using OP-U suspension and a velvet polishing cloth on the Imptech 30 DVT machine (Step 10). The slides were place on layers of the paper towel to ensure dryness as water could affect the bone collagen and cause the mounted specimen to detach from the slide.

Bone histo-morphometry and microanatomy

For the bone histo-morphometry, images of the complete bone section were captured using a Nikon digital camera attached to a stereomicroscope (Nikon SMZ745T). All the measurements were obtained using the ruler option in the NIS Element 3.0 software. For the sake of accuracy, a total of six measurements were taken at three levels on the section, because the sections are not circular and the bone wall has an uneven thickness (Table A4; Figure 5). The averages for the diameter of the section and the diameter of the medullary cavity were calculated. The bone cortical thickness (inversely proportional to the extent of the medullary cavity) was measured using the *k* index as coined by Currey and Alexander (1985). The *k* value is calculated by dividing the average diameter of the medullary cavity by the average diameter of the section. The *k* values lies between 0 and 1 whereby the closer to 0, the thicker the cortex and nearer to 1, the thinner the bone wall. Intra-specific comparisons between the *k* values (Table A5) of the bones in our sample were made in the form of descriptive statistics and box-and-whiskers graphs (Statistica 7) were plotted to illustrate the differences between both species.

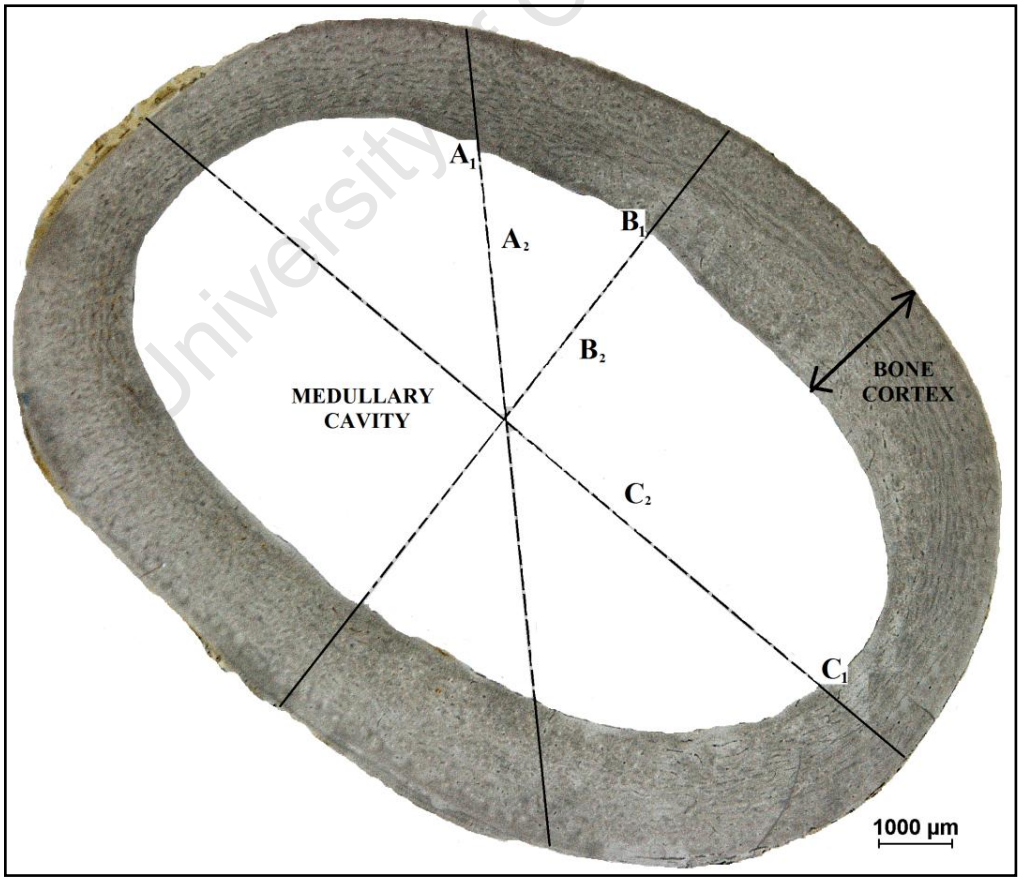

Figure 5: Approximate positions at which measurements have been taken to determine the bone cortical thickness (Example of the midshaft cross-section of the humerus of specimen G24). A_1, B_1 and C_1 (continuous + dotted lines) represent diameter of the cortex and the medullary cavity length. A_2, B_2 and C_2 (break lines only) represent the radius of the medullary cavity. The bone cortical thickness, or the *k* index (Currey and Alexander, 1985) has been calculated as follows: $k = ((A_2 + B_2 + C_2)/3) \div ((A_1 + B_1 + C_1)/3)$.

Bone histology

The bone histology deals with the description of the vascularization, the bone tissue type in the cortex, as well as the organization in layers on the bone wall (Figure 6). The layers that can be generally encountered in the long bone cortex of modern birds are usually the outer circumferential layer (OCL), the mid-cortex and the inner circumferential layer (ICL) (Ponton et al, 2004). The mid-cortex can vary in term of bone matrix type, which can be lamellar (highly organized tissue as a result of slow deposition of collagen fibers) or rather woven (highly disorganized due to fast, loose and random deposition of collagen fibers) (Currey, 2003). The vascularization can also vary, depending on the organization of the vascular canals and the type of vascular canals. The common types of vascularization present are simple vascular canals, primary osteons and secondary osteons (also known as Harvesian canals). When radially-oriented vascular canals inter-connect, they are known as Volkmann's canals (Padian and Lamm, 2013). The orientation of the vascularization can be circumferential, longitudinal, radial and reticular (Figure 7) (de Margerie et al, 2005). The presence of primary osteons with a woven bone tissue is referred to as fibrolamellar bone (de Ricqlès et al, 1991).

For the bone microanatomy and histological description, images were obtained using a Nikon digital camera mounted on a light compound microscope (Nikon Eclipse E200) and a stereomicroscope (Nikon SMZ745T) under normal and polarized light. The magnifications for the pictures under the stereomicroscope ranged from 10× to 50×. Under the compound microscope, the magnifications of the pictures ranged from 40×, 100× and 400× and the imaging software used was NIS Elements 3.0 (Nikon Instruments Inc.). The following qualitative and quantitative features were recorded to describe bone microstructure (Figure 6; Table A6-A7): a. Bone wall thickness. b. Description of the medullary cavity. c. Description of the circumferential layers. d. Bone tissue type in the mid-cortex. e. Type of vascularization in the mid-cortex (Figure 7)

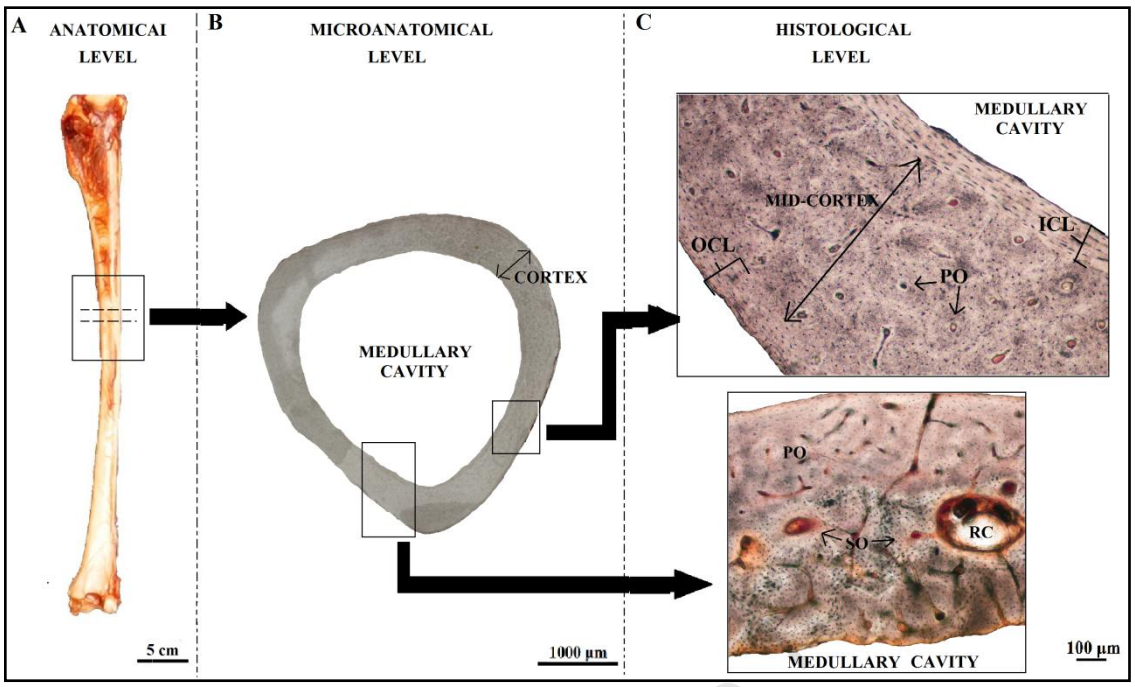

Figure 6: In the present work, the bones were studied at different levels of integration. From the left to the right: A. the anatomical level (measurements of the bones recorded before sectioning); B. the microanatomical level (the bone wall thickness was measured); C. the histological level (the bone cortical tissue was described). Abbreviations, OCL: outer circumferential layer; ICL: inner circumferential layer; PO: primary osteons; SO: secondary osteons; RC: resorption cavity.

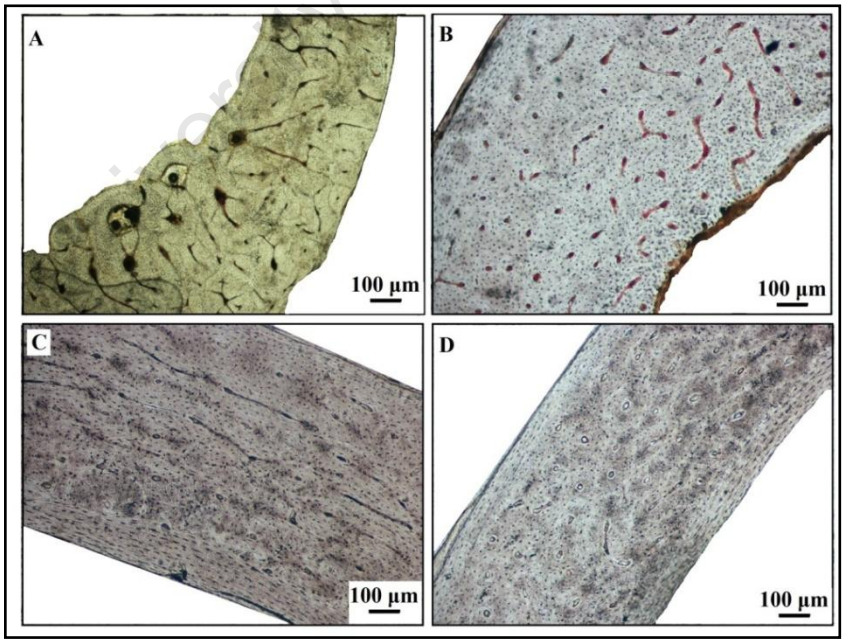

Figure 7: Diagram showing the various types of vascularization encountered in the bone slides and in modern birds in general. All sections are seen under normal light. A. Mostly radial. B. Reticular. C. Circumferential. D. Longitudinal.

RESULTS

Microanatomical and histological differences in the bone structure are well defined between the gannets and penguins allowing for inter-specific comparisons. Intra-specific bone variability was also observed thus denoting that some micro-structural differences occur within the ontogenetic stages, the genders of the individuals, and between the fore- and hind limb bones.

Bone wall thickness

Based on the *k* values obtained in this study, the results show that the penguins have thicker and more compact bones (low *k* values) as compared to the gannets which possess bones with a thinner and less compact structure (high *k* values) (Table A5; Figure 8; Figure 9). All comparative bone wall thickness is illustrated in Figure 8 that depicts the cross-sections of the different bones. A difference can be seen in the k values between adult penguins and adult gannets as depicted in the box-plots of the fore-limb bones and hind limb bones in Figure 9.

From this analysis, it can be seen that gannets exhibiting bimodal locomotion have a rather identical *k* values between the different fore-limb and hind limb bones sampled, with overlapping confidence intervals at 95% as they make use of both forewing and hindleg during diving. The *k* values for the fore-limb and hind limb bones of the adult gannets do not differ with a standard deviation that does not exceed 0.05 hence the homogeneity of the *k* values. There is an average *k* value of 0.73 for the humerus, radius, carpometacarpus and tarsometatarsus whilst the ulna, femur and tibiotarsus lie within a *k* value of 0.77 (Table A8). The *k* values for juvenile fore-limb and hind limb bones also do not differ with a variation that lies below 0.06 (Table A8). The fore limb bones and the hind limb stylopod of the juveniles have an average *k* value of 0.76 and both the hind limb zeugopod and the autopod have a mean *k* value of 0.72. Comparisons between the adults and juveniles *k* value averages for each bone results in the hind limb autopod having the same *k* (0.72). Only the hind limb zeugopod bears an ontogenetic *k* difference of 0.04 (juvenile tibiotarsus: 0.72, adult tibiotarsus: 0.76). All the other bones have a relatively small *k* value difference of 0.02 between adult and juvenile. The fore-limb and hind limb bones of the male and female gannets show deviation of less than 0.05 (Table A8). All the bones with the exception of the ulna and carpometacarpus differ by 0.02 between males and females.

The flightless penguin exhibit heterogeneous *k* values with large separate confidence intervals at 95% between the forewing and hindleg bones. The adult penguin bones show high differences as the fore-limb and hind limb bones deviate by a *k* value of 0.18 (Table A8). The fore limb bones are more compact than the hind limb bones with *k* values on averages 0.23 and 0.43 respectively. The juvenile penguin bones exhibit the same tendency as the adult with a difference in *k* value of 0.16 between hind limb and forelimb (Table A8). The average *k* value for the fore limb bones is 0.17 against 0.33 for the hind limb bones. There is a difference between adult and juvenile penguin fore-limb and hind limb bones. There was no difference between the fore-limb autopod of the juvenile and the adult (0.03). The fore-limb zeugopod and hindlimb stylopod differed by 0.07 between adult and juvenile. The most difference occurred in the humerus, tibiotarsus and tarsometatarsus with an average *k* value difference of 0.11 with adult having the higher *k* values. The fore-limb and hind limb bones of the male and female show little deviation of less than 0.19 (Table A8). The *k* values are small on average by 0.09 for all the fore-limb and hind limb bones of the female penguin (except for the ulna) as compared to the male penguins. This shows that the female fore-limb and hind limb bones are less compact than those of the males.

Microanatomical and histological description

African penguin

Hatchling: Only one penguin hatchling specimen (064) was available for histological and microanatomical analyses. All the fore-limb and hind limb bones appeared to have similar histological characteristics when examined under the microscope in normal and polarized light. The bones are all very compact (Figure 10a-11a). A reduced medullary cavity (m) is present and is not visible under the stereo-microscope but slightly visible under the compound microscope as it is almost entirely in-filled with bone trabeculae. The outer and inner circumferential layers, generally encountered in sub-adult or adult birds, are absent or if present, they are barely visible (Figure 10b-11b). The deep cortex (close to the medullary cavity) is composed of a highly vascularized fibrolamellar bone with longitudinal primary osteons (PO). The second half of the cortex is composed of large vascular canals (SVC) with a radial orientation with few longitudinal poorly-established primary osteons. The cortex is mostly formed of a woven bone matrix, characteristic of fast deposited bone tissue, with numerous, globular and disorganized osteocytes. This fibrous bone tissue, with a high vascularization is characteristic of hatchling individuals.

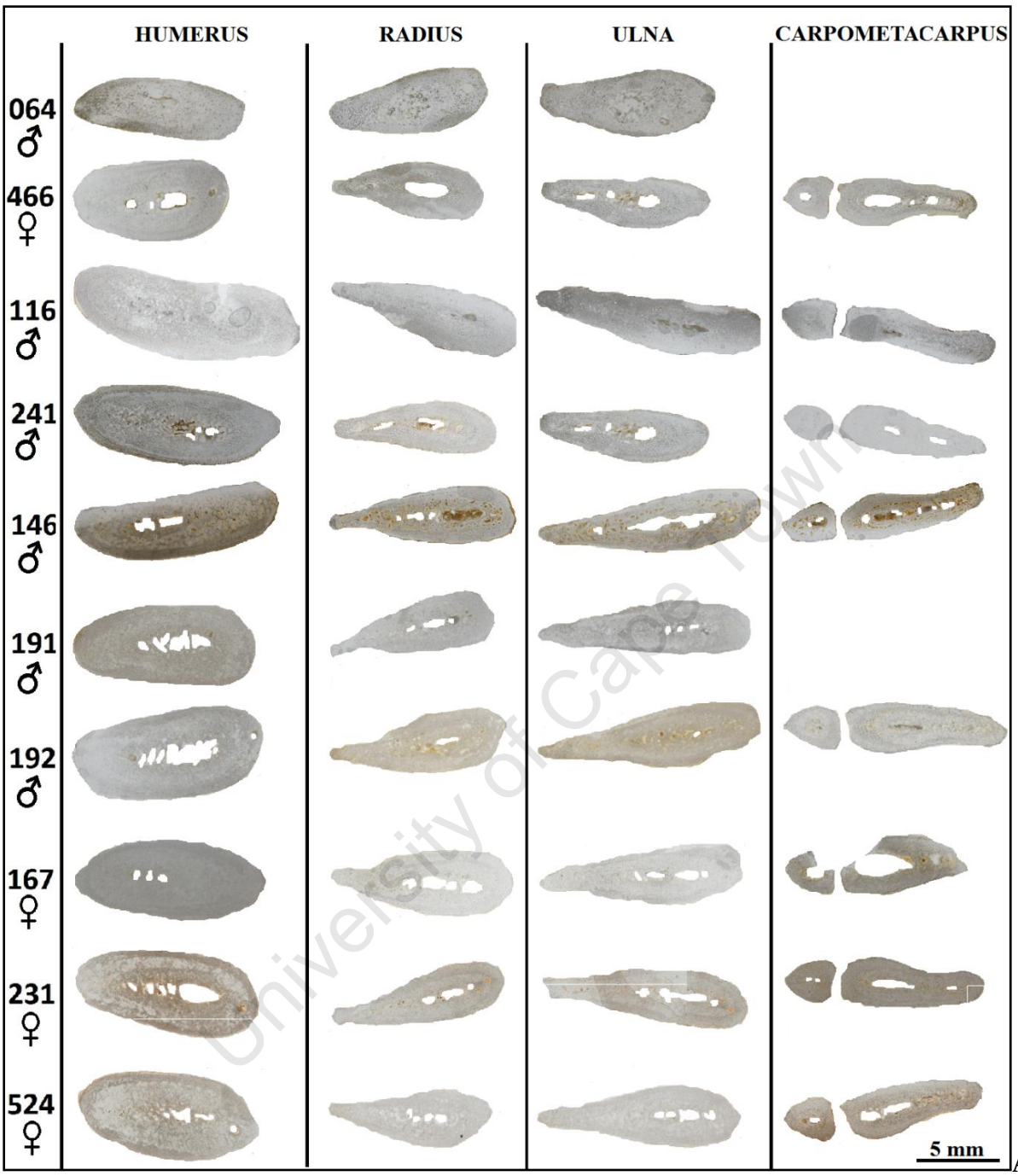

A.

Figure 8. A. The complete cross-sectional diagram of the fore-limb bones of the African penguin (*Spheniscus demersus*).

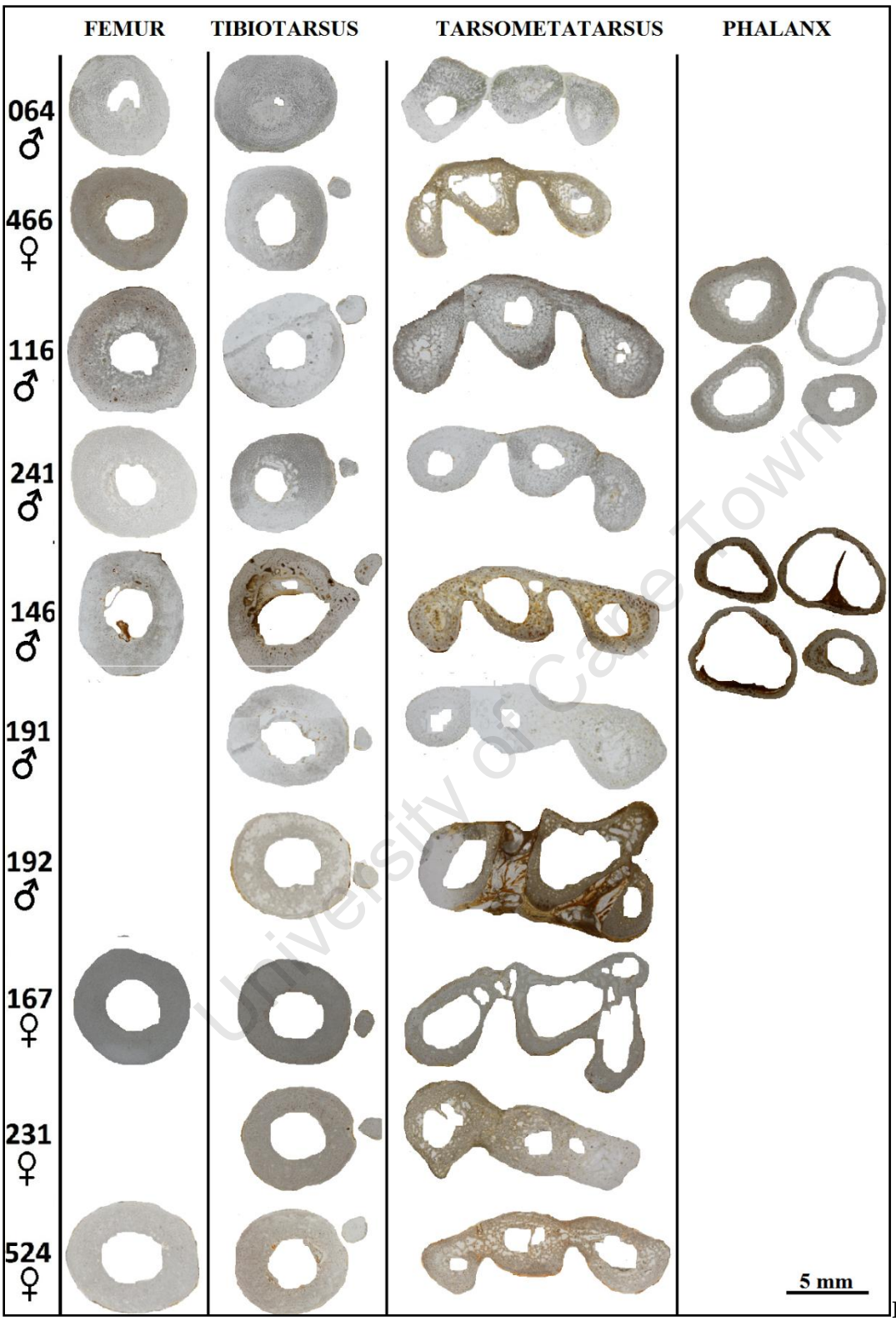

Figure 8. B. The complete cross-sectional diagram of the hind limb bones of the African penguin (*Spheniscus demersus*).

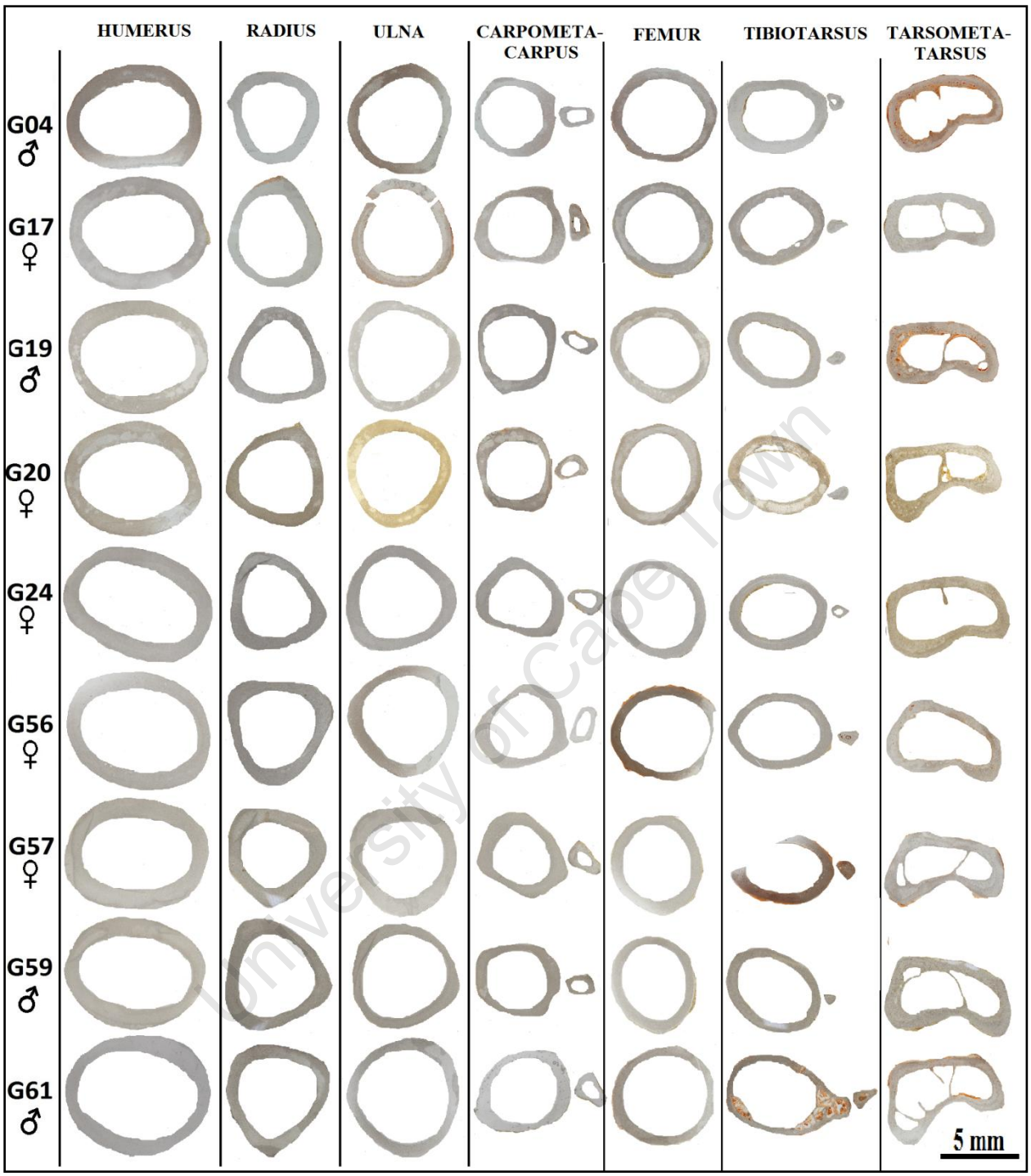

C.

Figure 8. C. The complete cross-sectional diagram of the fore-limb and hind limb bones of the Cape gannet (*Morus capensis*).

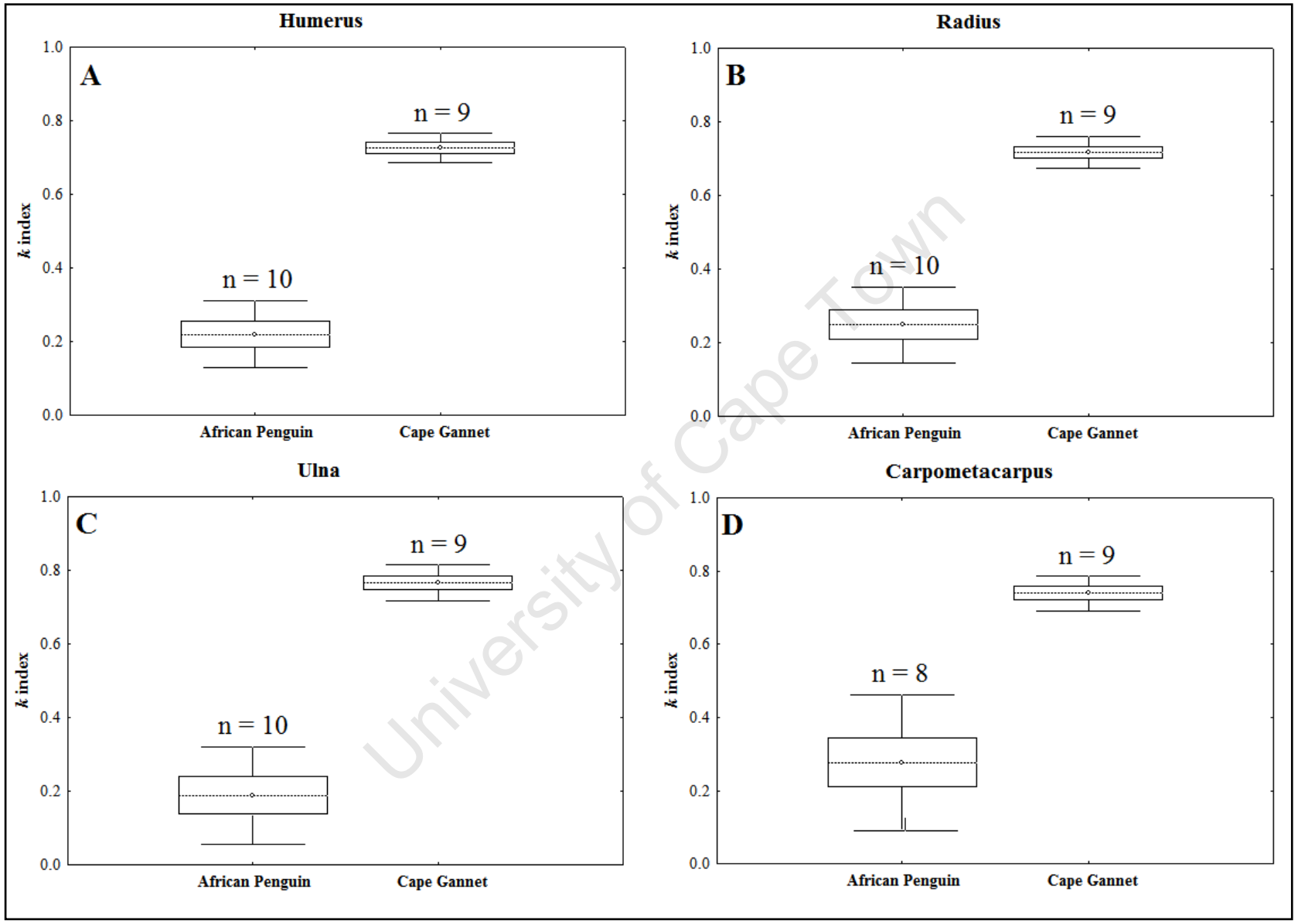

A.

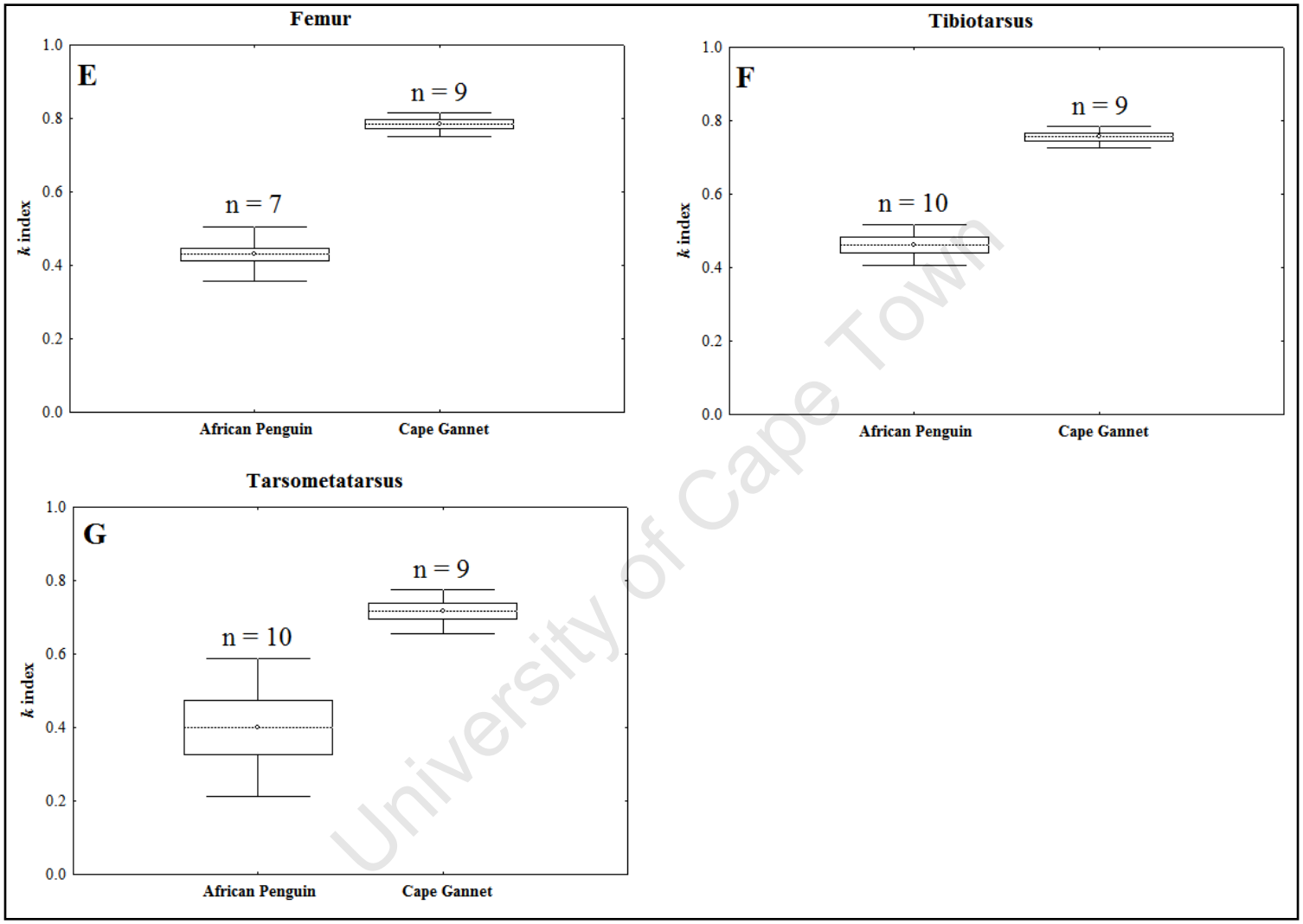

Figure 9: A. Box and whiskers comparative plots for the fore-limb bones of adult gannet and penguin using the *k* index values at CI: 95%. (A: Humerus; B: Radius; C: Ulna; D: Carpometacarpus). B. Box and whiskers comparative plots for the hind limb bones of adult gannet and penguin using the *k* index values at CI: 95%. (E: Femur; F: Tibiotarsus; G: Tarsometatarsus).

Juveniles: The three juvenile specimens appear to share similar microanatomical features. The bones are very compact with a more distinct medullary cavity as compare to the hatching medullary cavity (Figure 10c,e-11c,e) and some parts of the medullary cavity is filled up by trabecular bone. The outer circumferential layer is absent to partially present in some fore-wing bone and absent in all hind leg bones. The inner circumferential layer is barely noticeable. The four types of vascularizations namely circumferential, longitudinal, radial and reticular are encountered in the fore-limb and hind limb bone matrices (Figure 7). Primary osteons (PO) dominates the mid-cortex in a woven bone matrix, forming a highly vascularized fibrolamellar bone complex (Figure 10d,f-11d,f). In some sections, some small vascular canals (SVC), secondary osteons (SO) and resorption cavities (RC) can also be encountered closer to the medullary cavity.

Adult: The fore-limbs bones of the adult penguins all bear the same traits (Figure 12-13). The bone wall is thick and very dense and a well-defined medullary cavity can be observed at the center of the bone (Figure 12a,c). The medullary cavity is free of bone trabeculae. The outer circumferential layer is absent and the inner circumferential layer appears to be absent or poorly formed. Towards the medullary cavity in the mid-cortex, stratified layers are encountered. The outermost layer consists of poorly vascularized woven matrix consisting of primary osteons (Figure 12b,d). The second layer is dominated by longitudinal and reticular secondary osteons. The dominating layer closest to the medullary cavity is composed of few Harvesian canals with some Volkmann's canals with radial, longitudinal, reticular and few circumferential organization. Some resorption cavities can be encountered in some bones ((Figure 12b,d).

The bones of the hind limb are less compact with an even larger medullary cavity (Figure 13a,c). The periosteal layer is present and is thin, with flattened and well-organized osteocytes (Figure 13d). The endosteal layer is absent. The major types of vascularizations are radial and longitudinal with some reticulation (Figure 13b,d). The outer-cortex is composed of a layer of primary osteons in a woven bone matrix, followed by a zone of Harvesian canals in a deep cortex and a small number of resorption cavities lined with lamellar bone (Figure 13b,d).

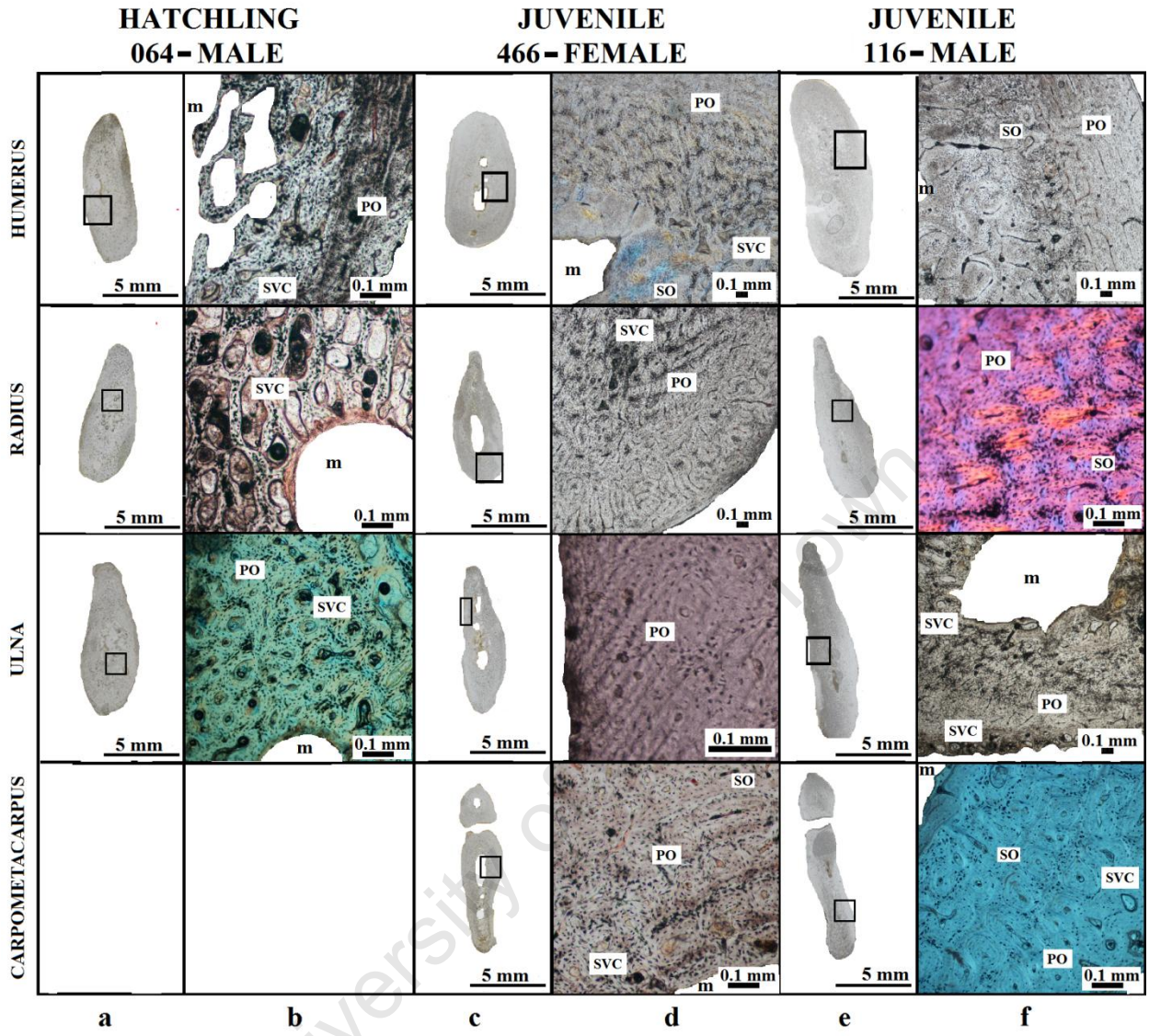

Figure 10: Comparative histology of the bones of the forelimbs of a male hatchling (specimen 064), female juvenile (specimen 466) and a male juvenile (specimen 116) African penguin. a, c and e are the complete cross-section of the bone cut at the mid-shaft region as seen under normal light. b, d, and f are the magnified view of the selected regions on the cross-section as seen under normal and polarized light. (m: medullary cavity; PO: primary osteons; SO: secondary osteons; SVC: simple vascular canal).

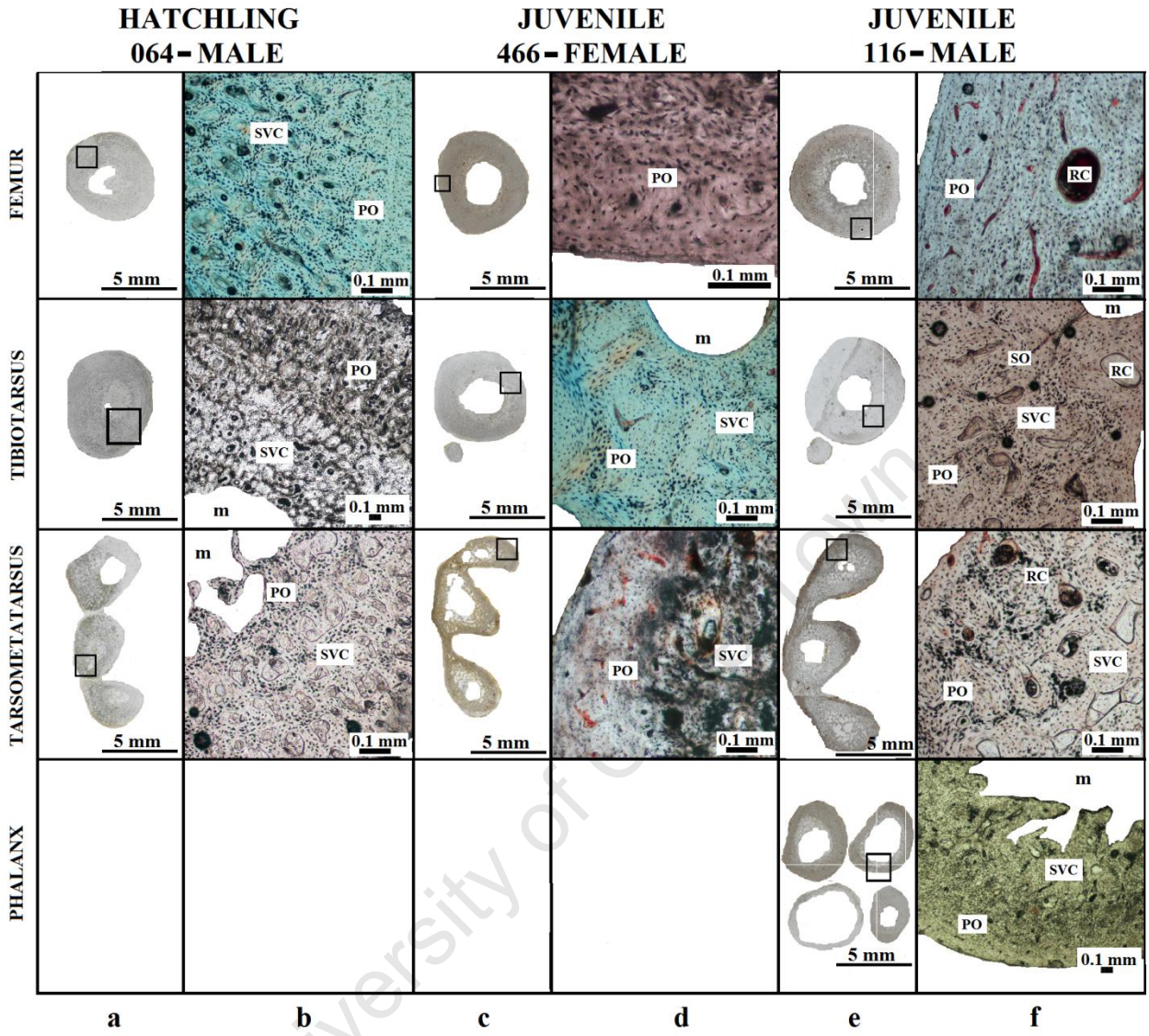

Figure 11: Comparative histology of the bones of the hind limbs of a male hatchling (specimen 064), female juvenile (specimen 466) and a male juvenile (specimen 116) African penguin. a, c and e are the complete cross-section of the bone cut at the mid-shaft region as seen under normal light. b, d, and f are the magnified view of the selected regions on the cross-section under normal and polarized light. (m: medullary cavity; PO: primary osteons; SO: secondary osteons; SVC: simple vascular canal; RC: resorption cavity).

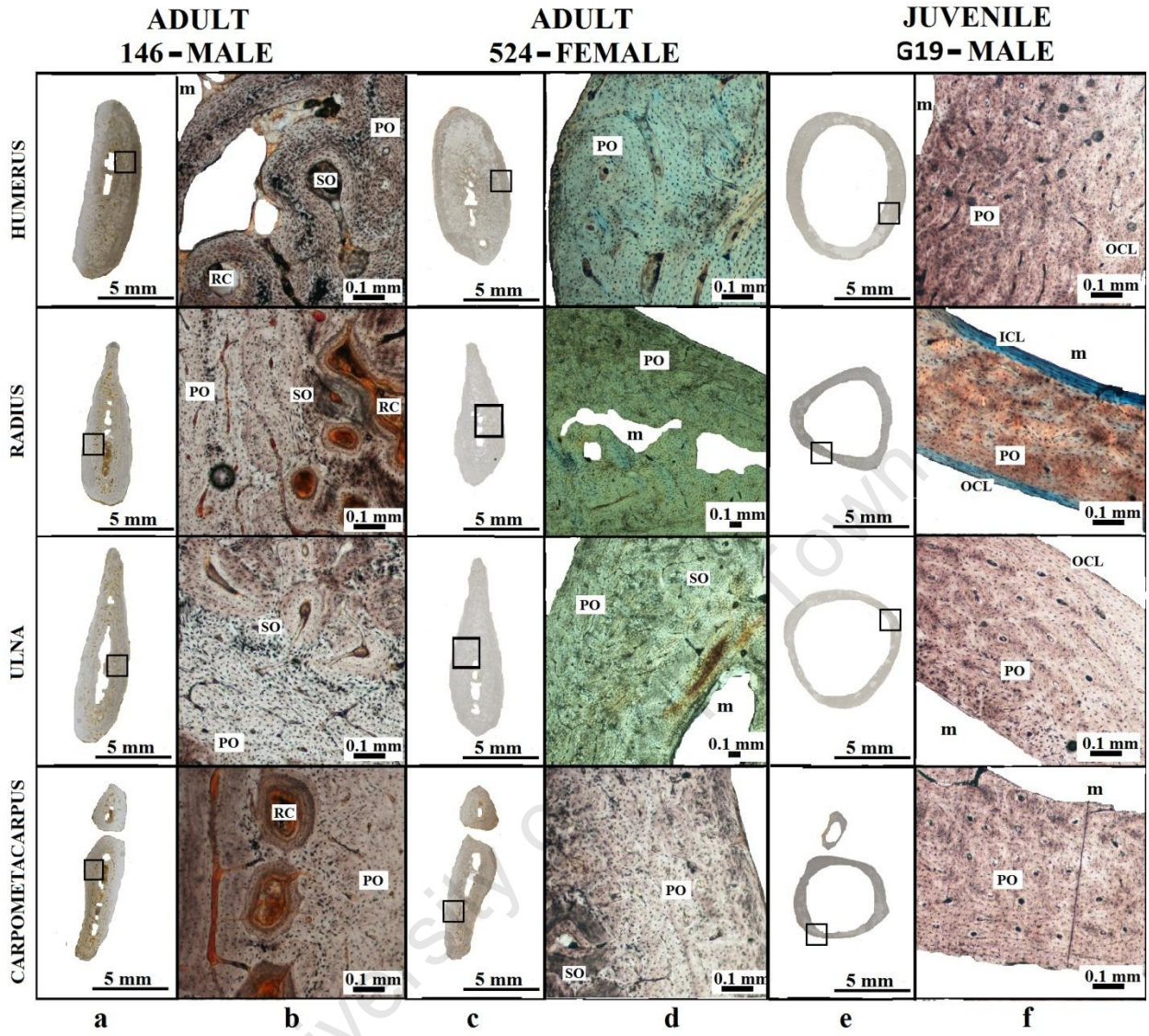

Figure 12: Comparative histology of the bones of the forelimbs of a male adult (specimen 146) and female adult (specimen 524) African penguin and a male juvenile (specimen G19) Cape gannet. a, c and e are the complete cross-section of the bone cut at the mid-shaft region as seen under normal light. b, d, and f are the magnified view of the selected regions on the cross-section under normal and polarized light. (m: medullary cavity; PO: primary osteons; SO: secondary osteons; RC: resorption cavity; OCL: outer circumferential layer; ICL: inner circumferential layer).

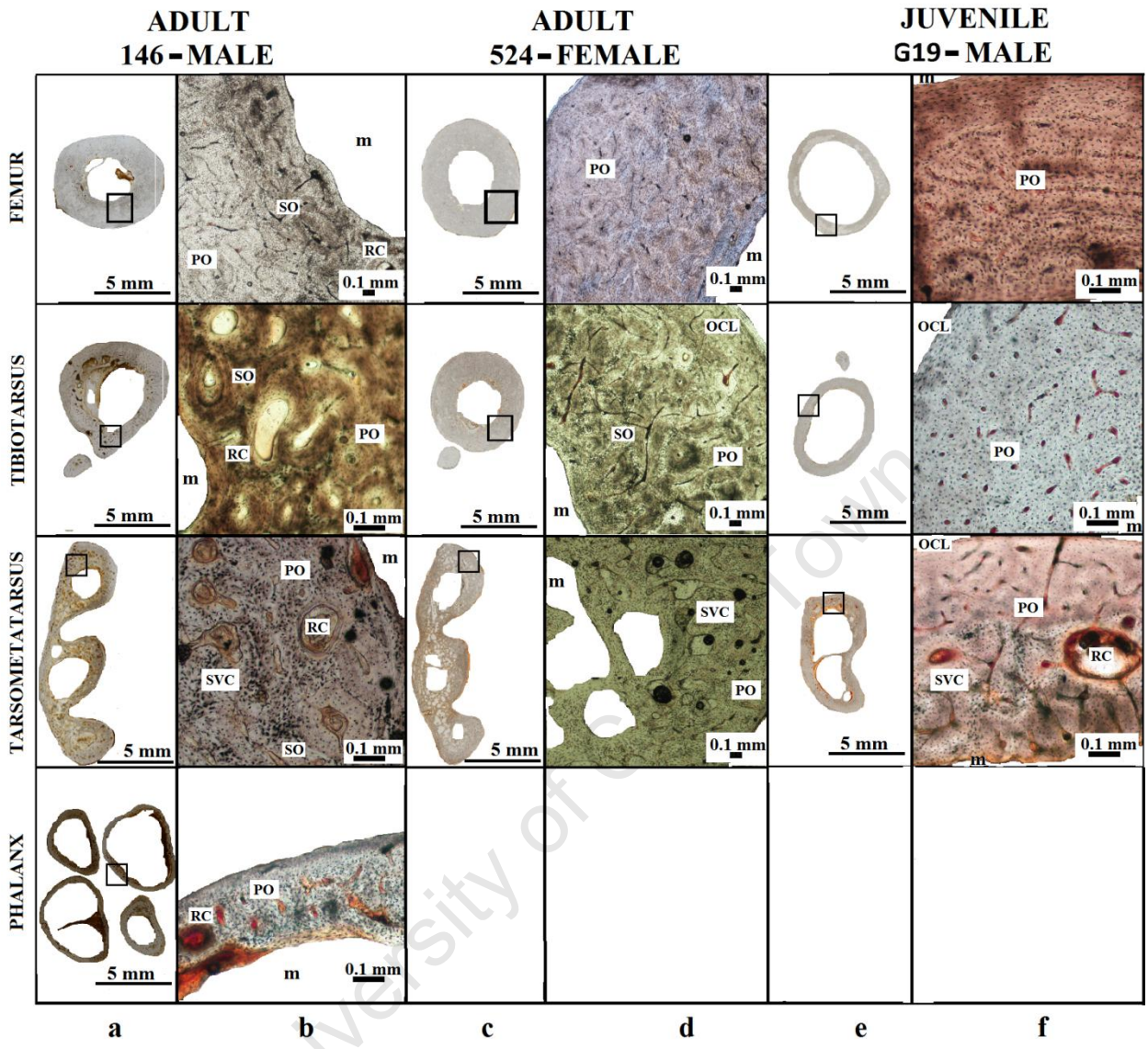

Figure 13: Comparative histology of the bones of the hind limbs of a male adult (specimen 146) and female adult (specimen 524) African penguin and a male juvenile (specimen G19) Cape gannet. a, c and e are the complete cross-section of the bone cut at the mid-shaft region as seen under normal light. b, d, and f are the magnified view of the selected regions on the cross-section under normal and polarized light. (m: medullary cavity; PO: primary osteons; SO: secondary osteons; RC: resorption cavity; OCL: outer circumferential layer; SVC: simple vascular canal).

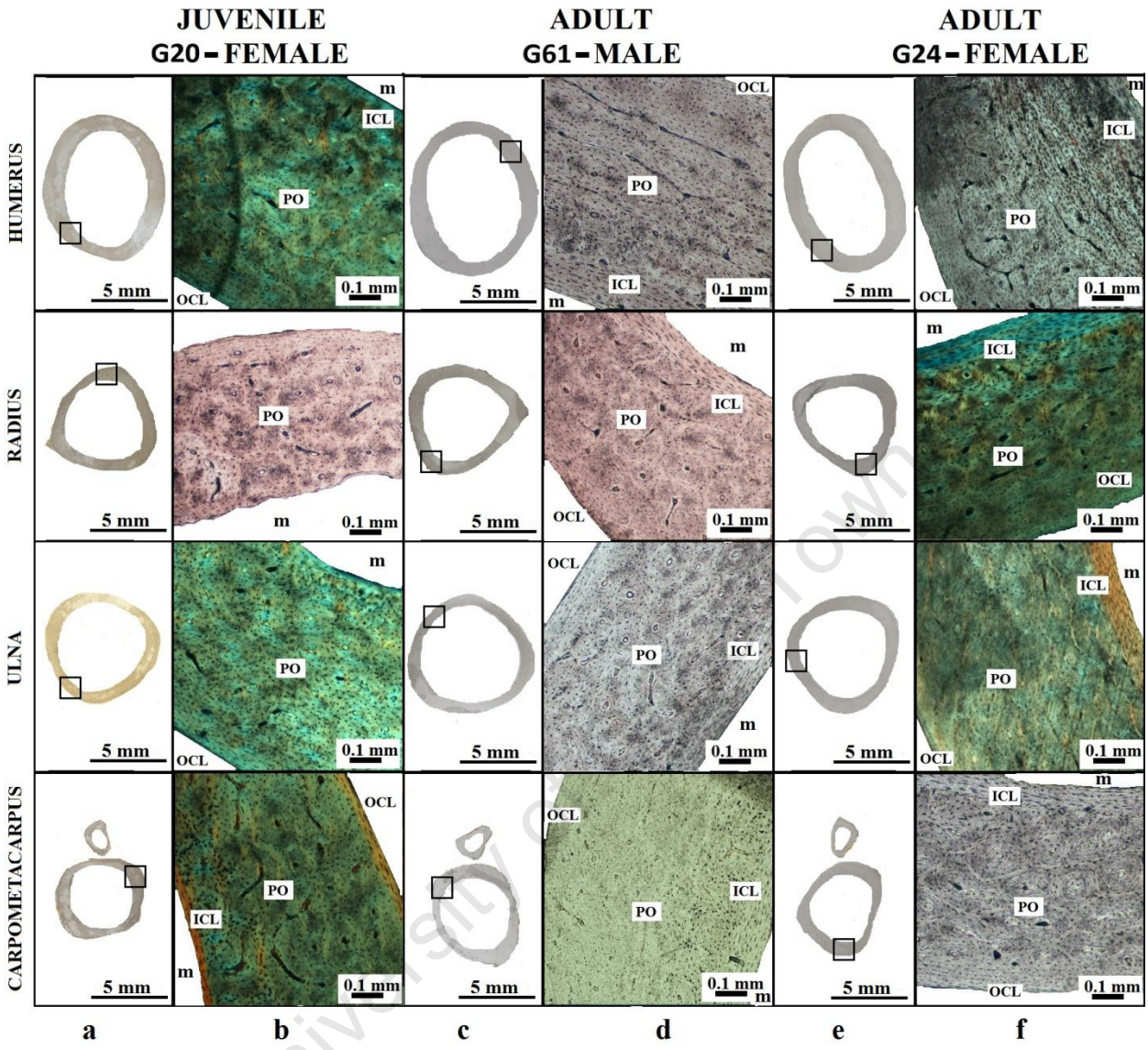

Figure 14: Comparative histology of the bones of the forelimbs of a female juvenile (specimen G20), male adult (specimen G61) and a female adult (specimen G24) Cape gannet. a, c and e are the complete cross-section of the bone cut at the mid-shaft region as seen under normal light. b, d, and f are the magnified view of the selected regions on the cross-section as seen under normal and polarized light. (m: medullary cavity; PO: primary osteons; OCL: outer circumferential layer; ICL: inner circumferential layer).

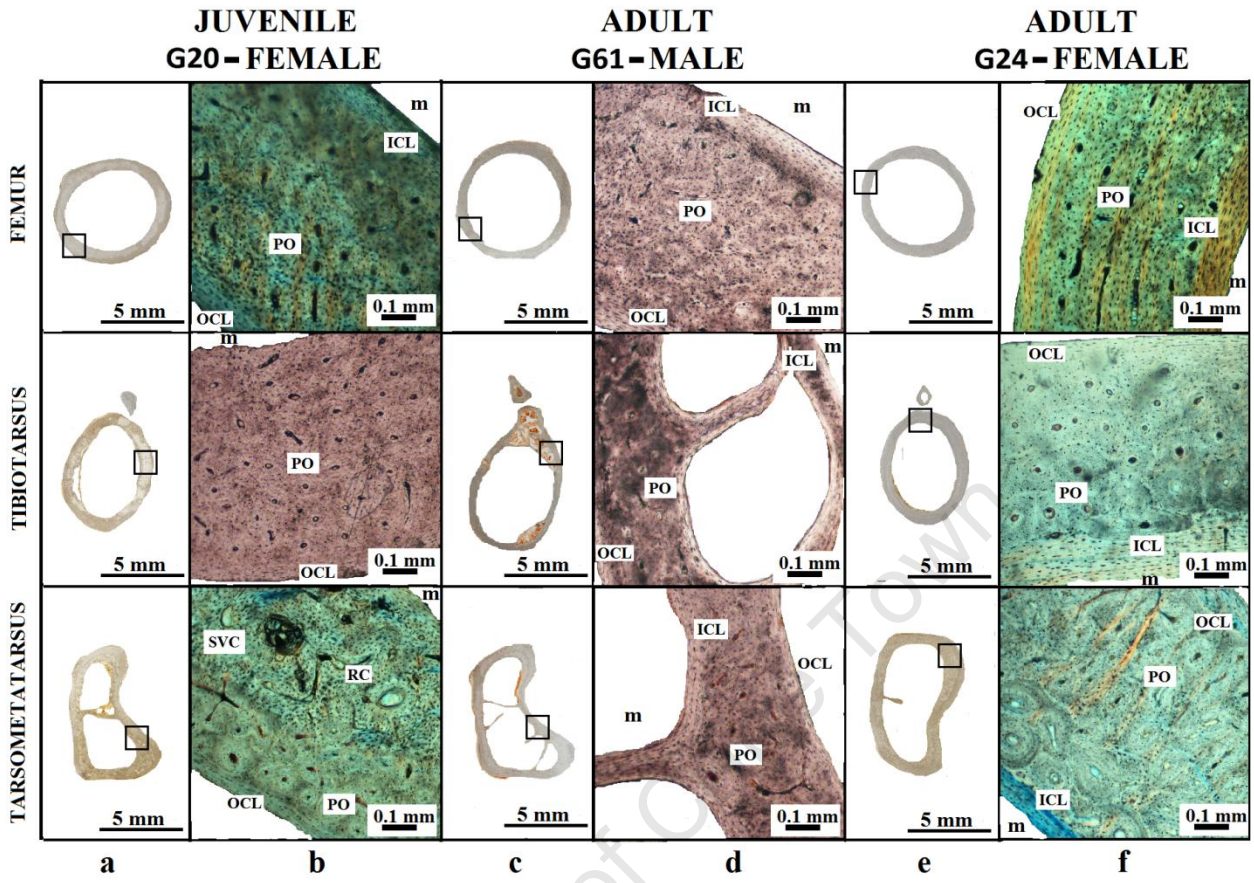

Figure 15:: Comparative histology of the bones of the hind limbs of a female juvenile (specimen G20), male adult (specimen G61) and a female adult (specimen G24) Cape gannet. a, c and e are the complete cross-section of the bone cut at the mid-shaft region as seen under normal light. b, d, and f are the magnified view of the selected regions on the cross-section under normal and polarized light. (m: medullary cavity; PO: primary osteons; SVC: simple vascular canal; RC: resorption cavity; OCL: outer circumferential layer; ICL: inner circumferential layer).

Cape gannet

Juvenile: The juvenile gannet bones are less compact as compared to the penguin bones, having a thin bone cortex with a large medullary cavity (Figure 12e, 13e, 14a, 15a). A well-defined outer circumferential layer runs around the bone, suggesting that the active growth phase is over and that the growth slowed down ((Figure 12f, 13f, 14b, 15b). The inner circumferential layer is however less pronounced and incomplete ranging from being absent to thin and to thick layer in some parts of the section. The mid-cortex is composed of numerous primary osteons set in a woven bone matrix with longitudinal and reticular orientation (Figure 12f, 13f, 14b, 15b). Additionally, the tarsometatarsus is the only bone to feature resorption cavities ((Figure 12f, 13f, 14b, 15b).

Adult: All adult gannet bones have a large medullary cavity surrounded by a thin bone wall (Figure 14c,e-15c,e). The bone compacta is made up of a distinct thin outer circumferential layer in the outermost region (Figure 14d,f-15d,f). The mid-cortex is fibrolamellar and bears numerous and mostly longitudinal primary osteons in a woven matrix (Figure 14d,f-15d,f). The inner circumferentiallayer, surrounding the medullary cavity, is very thick (Figure 14d,f-15d,f). The types of vascularization that dominates the cortex are longitudinal and reticular (Figure 7b-d). Circumferentially-oriented vascularizations occurs in the humerus, ulna and femur (Figure 7c).

Intra-specific variability

In the juvenile penguin specimens, one specimen (241) appears to possess numerous large simple vascular canals radiating from the medullary cavity and lining the outermost layer of the bone section (Figure 16a). One adult penguin bones (146) bears numerous resorption cavities (Figure 16b). The bones of one gannet bird (G56) possess resorption cavities and secondary osteons amidst fibro-lamellar bone (Figure 16c).

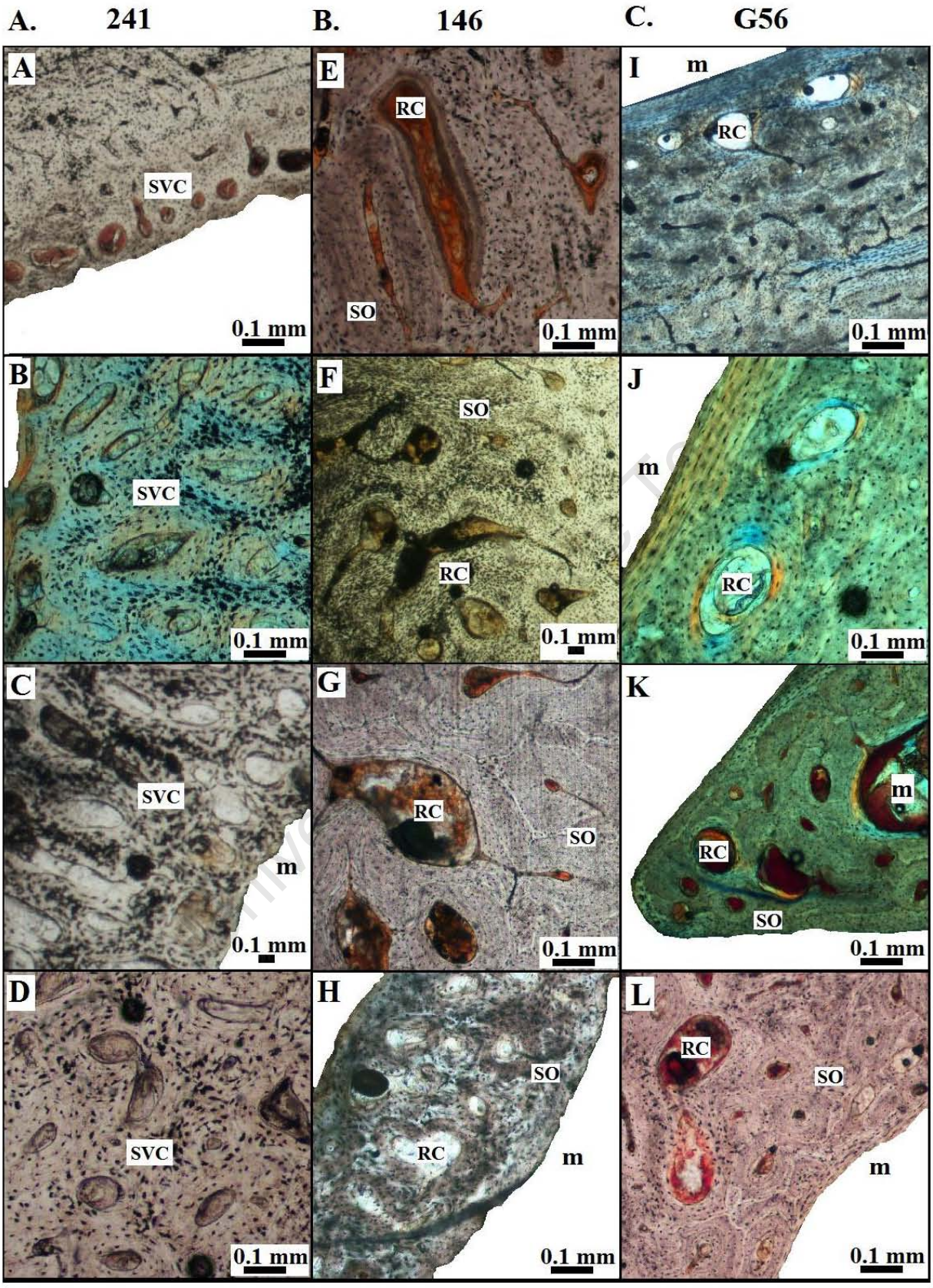
A. 241
B. 146
C. G56
A
SVC
0.1 mm
E
RC
SO
0.1 mm
I
m
RC
0.1 mm
B
SVC
0.1 mm
F
SO
RC
0.1 mm
J
m
RC
0.1 mm
C
SVC
m
0.1 mm
G
RC
SO
0.1 mm
K
m
RC
SO
0.1 mm
D
SVC
0.1 mm
H
SO
RC
m
0.1 mm
L
RC
SO
m
0.1 mm

Figure 16. Intra-specific bone differences as exhibited by some specimens. A. Juvenile African penguin specimen 241 possesses numerous vascular canals in the cross-sections of its limb bones. [A. Humerus. B. Tarsometartarsus. C. Ulna. D. Tibiotarsus]. B. Adult African penguin specimen 146 possesses large resorption cavities and some secondary osteons in itsbones. [E. Carpometacarpus. F. Humerus. G. Tibiotarsus. H. Tarsometatarsus]. C. Cross-sectional diagram of various bones of the Cape gannet adult specimen G56 under normal and polarized light. All the sections of bones are showing secondary osteons and resorption cavities. [I. Humerus. J. Radius. K. Fibula which is fused to the tibia to form the tibiotarsus. L. Tarsometatarsus]. Abbreviations: m: medullary cavity; RC: resorption cavity; SO: secondary osteons; SVC: small vascular canals.

Ontogenetic variability

African penguin: Some ontogenetic differences can be noted in the organization of the bone compacta through ontogeny in *Spheniscus demersus*. The hatchling bears no inner or outer circumferential layers and the mid-cortex comprises of a woven bone matrix with a number of primary osteons and small vascular canals (Figure 10-11). The bone structure of the juvenile has primary osteons in a woven bone matrix and the presence of very few small vascular canals in the mid-cortex (Figure 10-11). The adult bone compacta is stratified with three distinctive layers when moving towards the bone cavity. The outer circumferential layer is visible in some bones. The layers include an outermost layer of fibrolamellar bone, a second layer of loosely arranged secondary osteons and lastly a layer composed of dense Harvesian canals closer to the medullary cavity (Figure 12-13).

Cape gannet: The ontogenetic variability in the juvenile and adult fore-limb and hind limb bones of *Morus capensis* are less pronounced. The juveniles have a thinner inner circumferential layer (Figure 14-15) whilst the adults possess a relatively thicker inner circumferential layer (Figure 14). Besides both having longitudinal and reticular vascularizations, the adults also have a number of circumferentially oriented canals (Figure 14-15). The tarsometatarsus of the juveniles differs such that they have resorption cavities, a feature absent in the adult leg bone (Figure 15).

Gender comparison

African penguin: The differences between the males and females are minimal. The female fore-limb and hind limb bones appear to have thicker inner and outer circumferential layers as compared those of the males. Some of the fore-limb and hind limb bones of the adult males possessed numerous resorption cavities; a feature absent in females.

Cape gannet: The structural distinction between gannet sexes is that females appear to have thinner inner and outer circumferential layers than males. Circumferentially oriented canals are only observed in some of the female gannet fore-limb and hind limb bones. Radially oriented canals are only seen in some of the male gannet fore-limb and hind limb bones.

The differences between the sexes of each species are not clearly evident. This may be due to the small sample size. There is also the possibility that the individuals did not fall within the same age range and therefore some of them may have been very old birds as indicated by the very thick inner and outer circumferential layers and the organization of the bone matrix (Age, Weight- Table A1).

Inter-specific differences

The most important difference between the penguin and gannet fore-limb and hind limb bones is the compactness. Penguins have a very compact fore-limb and hind limb bone structure with a small to nearly non-existent medullary cavity whilst the gannet fore-limb and hind limb bones are slender, thin-walled and bear a large hollow medullary cavity (Figure 17 –A and C). The penguin fore-limb and hind limb bones have well-defined stratified mid-cortical layers with numerous small vascular canals whilst the gannet fore-limb and hind limb bones are dominated by primary osteons. The presence of the inner and outer circumferential layers is more evident in the gannet fore-limb and hind limb bones being thicker and well-organized (Figure 17-B and D).

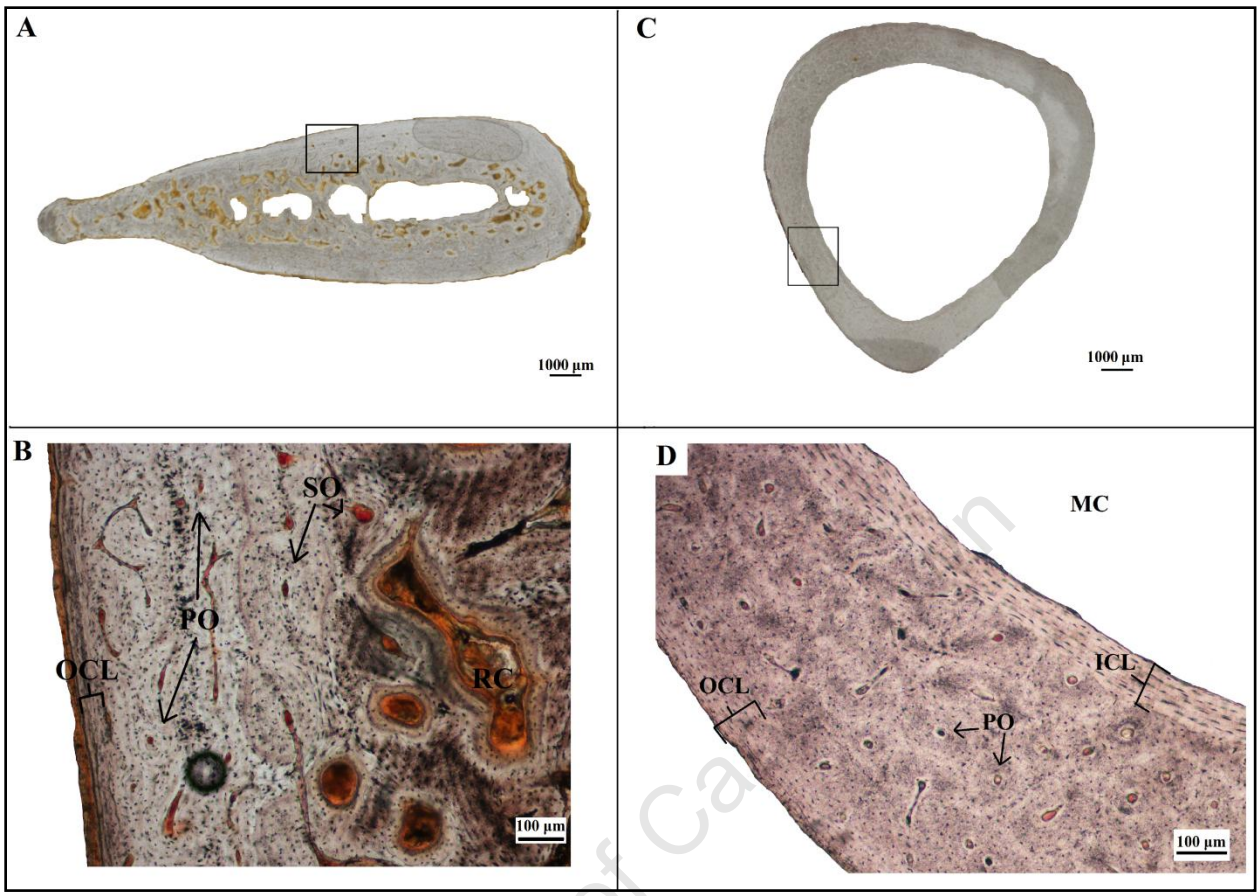

Figure 17: Comparative cross-sectional diagram of the radius of the African penguin (*Spheniscus demersus*) (146) and Cape gannet (*Morus capensis*) (G61). Both specimens are adult males. A. Cross section of the entire radius of the African penguin. B. Magnified view of the section. C. Cross section of the entire radius of the Cape gannet. D. Magnified view of the section. [ICL = inner circumferential layer; OCL = outer circumferential layer; PO = primary osteons; SO = secondary osteons; RC = resorption cavities; MC = medullary cavity].

DISCUSSION

The microanatomical and histological results obtained for the African penguin (*Spheniscus demersus*) and the Cape gannet (*Morus capensis*), indicates that intra- and inter-specific variability occurs within the same species and between species and between the fore-limb and hind limb long bones and that such differences relates to the ontogenetic stage and the gender of the individuals.

Intra-specific variability

Within the juvenile penguin, one specimen (241) is found to have a different micro-structure as compared to the two others indicative that this individual is still actively growing (Figure 16a- Results section). The trabecular bone filling up the medullary cavity is more pronounced in this particular individual. In terms of bone compactness, specimen 241 has a less compact fore-limb bone when compared to the fore-limb bone of the other two juvenile penguin specimens indicating that the fore-limb bones are the most affected during ontogenesis. The hind limb bones do not seem to be the most affected as all the individuals appear to have a homogenous bone wall thickness (Table A5).

One male adult penguin (146) appears to have been molting at the time of its death when compared to other male adult penguin individuals (Figure 16b-Results section). Since the other two male adult penguins were similarly larger and heavier (Head length and Weight-Table A1), it can be presumed that specimen 146 (which was smaller) was a sub-adult and that it was at the right age, size and weight to molt into an adult. As mentioned by Canoville (unpublished data), the stylopod and zeugopod bones of the King penguin (*Aptenodytes patagonicus*) are the most affected during molting. In specimen 146, the stylopod and the zeugopod bones of the fore-limb bones all have large resorption cavities. In the hind limb bones, since the zeugopod is the most affected. The zeugopod bones of the fore-limb and hind limb are less compact when compared to other individuals of the same age (Table A5); further confirming that these bones are the most affected during the molting phase.

The bones of one adult female gannet bird (G56) possess resorption cavities and secondary osteons (Figure 16c). Physiological stress like ovulation or starvation affects the calcium levels in bones. When calcium levels are reduced, this allows osteoclast to start resorbing (Dacke et al, 1993). This species was very thin and weighed less than the other adult female gannets. The bone micro-structure shows a high level of resorption occurring. Therefore, indicating that this bird was under a lot of physiological stress attributed to starvation caused by intestinal perforation before its death (Cause of death- Table A1). The stylopod, zeugopod and autopod of the fore-limb and hind limb bones of specimen G56 are less compact as compared to the other female gannets indicating that resorption occurred in all its bones (Table A5).

Inter-skeletal variability

Spheniscus demersus

From the analysis of the bone wall thickness (Table A8), it can be seen that the inter-skeletal elements develop at different rates during the ontogenetic stages of the African penguin. The pectoral bones mature slowly from hatchling to adult whilst the pelvic bones mature faster such that the juvenile penguin hind-limb bones are almost similar to the adult penguin hind-limb bones. Additionally, the different bones in the pectoral bones also mature at different rates with the stylopod maturing the fastest followed by the zeugopod and the autopod. Therefore, there is a trend in the maturation of the bones with the bone maturing faster going from the proximal to distal end of the fore-limb bones. Similarly, the pelvic bones have the same characteristics. The femur matures faster than the zeugopod and autopod and the tibiotarsus matures faster than the tarsometatarsus. The difference between the maturation of the fore-limb bones and hind-limb bones is explained by the fact that the hatching and the juvenile have a terrestrial locomotion at their young age and subsequently when they become adult, there is a change from terrestrial to a sub-aquatic locomotion. It can be noted that the fore-limbs bones are the most affected by sub-aquatic locomotion as the bone trabeculae is replaced by compact bone due to the increase in the thickness of the cortex; a condition known as osteosclerosis (Domning and de Buffrénil, 1991). The bone is less compact when moving from the proximal humerus to the distal tarsometarsus, a tendency similarly reported in the dugong (dugong dugon) (Buffrénil and Schoevaert, 1989).

Morus capensis

The k values of the Cape gannet bones shows that there is no difference between the long bone thickness between the juvenile gannets and the adults gannets (Table A8). This means that the gannet pectoral and pelvic bones already matures when the bird is still very young. In the juveniles, the fore-limb bones have a less compact bone structure than those of the hind limb bones which could be accountable by their terrestrial lifestyle. The juvenile fore-limb and hind-limb bones changes slightly as the individual matures into an adult with the fore-limb bones becoming more compact than the hind-limb bones which remains at the same thickness as the juvenile long bones. This is because the gannet changes its lifestyle from terrestrial to aerial and sub-aquatic and therefore there is an increase in the use of the fore-limb bones during flying.

Ontogenetic variability

Spheniscus demersus

There are some differences between the bone microstructure of the hatchling, juvenile and adult penguins. The hatchling fore-limbs and hind limb bones show that active growth phase is occurring as bone deposition is very fast and disorganized resulting in rapid extension of compact bone over the filling of the mid-cortex with primary osteon (de Margerie, 2004). The juvenile fore-limb and hind limb bones show that active growth has stopped. Osteosclerosis is taking place as the bone trabeculae in the juvenile fore-limb bones are slowly replaced by the compact bone. In the adult fore-limb and hind limb bones, the bone trabeculae is completely replaced by compact bone and therefore the bone wall thickness of the adult penguin increases. Adult penguins have a less compact bone as compared to hatchling and juvenile due to their lifestyle adaptation. Hatchling and juvenile are primarily terrestrial during the early stages of their life cycle. Therefore, when maturing into adults, their bones becomes more compact since land animals that have re-adapted themselves to an aquatic lifestyle bears osteosclerosic conditions (de Ricqlès and Buffrenil, 2001).

Morus capensis

The fore-limb and hind limb bones of the juvenile and adult gannet do not show much difference in the bone micro-structure. All the juvenile hind-limb autopod bone have some resorption cavities which is probably linked to the extensive usage of this bone during terrestrial locomotion when they venture out of their colonies and are therefore left to fend for themselves. According to Jarvis (1972), the young juveniles have 10 days to learn to forage otherwise they will starve to death. The presence of resorption cavities in the tarsometatarsus could be a result of physiological stress due to starvation; thus causing calcium to be relocated. Canoville (unpublished paper) has found the same pattern in the femur and/or the tibiotarsus of two adult King penguins (*Aptenodytes patagonicus*) which were attributed to physiological stress at the time of their death. The presence of circumferential canals in the mid-cortex of the humerus, ulna and femur of the adult gannet is related to their bimodal locomotion. These are the main bones used during flight and underwater propulsion under water as these bones all possess torsion-resistant features as described by de Margerie et al (2005). The laminarity of the bone combined with the low compactness and the large hollow medullary cavity of the bone wall confers properties that allows for buoyancy and waterdrag control when underwater.

Inter-specific variability

The Cape gannet fore-limb and hind limb bones have a large hollow medullary cavity and a thin-walled cortex which is relative to the findings of other sub-aquatic birds with bimodal locomtion by Habib and Ruff (2008). De Margerie et al. (2005) attribute this to the biomechanical adaptation to flying since the humerus, ulna and femur micro-structural properties confer torsional resistance. In contrast, the flightless African penguins, which are exclusively aquatic in their adult phase, possess very compact bone due to partial osteosclerosis of the medullary cavity. This coincides with the findings in other exclusive marine birds like the *Hesperornis regalis* (Chinsamy et al, 1998) and the *Phalacrocorax harrisi* (Habib and Ruff, 2008).

Physiological implications

Morus capensis

As seen in the foraging behaviour of the Cape gannet (previously described in the Material and methods section), these birds travel far distances at sea to reach their feeding sites (Grémillet et al, 2004). Therefore, an efficient flying apparatus is needed to achieve long-distance travel. The thin-walled bones and the type of vascularizations confers structural properties that is torsion-resistant against wind pressure on their wings especially since the air current above the ocean can be very unpredictable (de Margerie et al, 2005). Furthermore, this species exhibit both flying and aquatic locomotion (Ashmore, 1971). Cape gannets plunge-dive into the ocean to catch their prey and when into the water, they use both forelimbs and hind limbs for underwater propulsion. However, previous studies have shown that the gannets do not dive very deep; they dive to about 3.6 metres into the water due to their low breathing retention time of 4.3 seconds (Grémillet et al, 2004; Ropert-Coudert et al, 2004). This implies that gannets must have a way to control their buoyancy so as to ensure that they stay close to the surface in the water column. The presence of a large medullary cavity and less compact bones provides buoyancy to some extent as it decreases the overall body mass of the birds.

Spheniscus demersus

African penguins exhibit sub-aquatic locomotion by means of fore-limbs propulsion underwater. Penguins dive deeper than the Cape gannets (average 17 meters) and remain underwater far longer (2.5 minutes) (Wilson and Wilson, 1995). Since penguins dive so deep, a large amount of energy is required by the muscles to overcome such water pressure (Schmidt-Nielsen, 1997). The hind limbs are especially adapted for such deep diving. The flattened morphology of the bones offers low resistance to movement in the water. This provides an efficient way to conserve energy. In order to dive to such depths, penguins need to be heavy enough to reduce buoyancy. Therefore the medullary cavity is greatly reduced so as to reduce the air spaces which promote buoyancy. The high level of compactness of the bone wall provides weight to the skeletal structure.

CONCLUSION

There is a definite difference between the microanatomy and histology of the fore-limb and hind limb bones of the African penguin (*Spheniscus demersus*) and the Cape gannet (*Morus capensis*) based on their aquatic lifestyle adaptations and the type of locomotion. The ontogenetic stage of the species greatly affects the bone micro-structure. In the penguins, the bone compactness increases with maturation of the birds. In the gannets, the juvenile bones have the same bone wall thickness as the adult suggesting that the bone matures very fast. Some individuals exhibit intra-specific variability due to physiological stresses (active growth, molt, injuries). Inter-skeletal variability occurs in the fore-limb and hind limb bones across the stylopod, zeugopod and autopod with the stylopods and zeugopods being the bones that are most affected by sub-aquatic locomotion.

To further prove that aquatic lifestyle adaptation and the type of locomotion affects the bone micro-structure, the inclusion of another species is essential. The most appropriate species is the Cape cormorant (*Phalacrocorax capensis*) as this species also exhibit bimodal locomotion just like the Cape gannet, but unlike the African penguin which is a fore-limb propelled diver, this species is a hind limb propelled diver. Additionally, a more in depth studies could be achieved pertaining to the intra-specific gender differences of the species with the addition of a bigger number of males and females in the biological sample. Particular attention should be given in future studies into the possible presence of lines of arrested growth (LAGs) in the bone cortex, an important ontogenetic feature that was not observed in our sample and yet have been found in numerous bird species in other studies. In order to gain a complete understanding of the interspecific and intraspecific differences of the birds in this study, an accurate examination of the bird foraging behaviour and life-cycle with relation to physiological implications of the bone micro-structure should be conducted. Only after these aims have been fulfilled, a more in depth comprehension into the effect of the micro-structure of long bones of marine aquatic birds with respect to their aquatic adaptations would be promising.

REFERENCES

Literature cited:

Ashmole NP. 1971. Seabird ecology and the marine environment. In Farner, D.S. & King, J.R., eds. Avian Biology. Vol 1. New York, *Academic Press*, 112–288.

Buffrénil V de, Schoevaert D. 1989. Données quantitatives et observations histologiques sur la pachyostose du squelette du dugong, *Dugong dugon* (Müller) (Sirenia, Dugongidae). *Canadian Journal of Zoology*, 67: 2107–2119.

Canoville A. Thesis. Unpublished. Ontogenetical development of long bone microanatomy and histology of the King Penguin (*Aptenodytes patagonicus*, Miller, 1778) in relationship with its aquatic adaptation.

Chinsamy A, Raath MA. 1992. Preparation of fossil bone for histological examination. *Palaeontologia Africana*, 29: 39-44.

Chinsamy A, Martin LD, Dodson P. 1998. Bone microstructure of the diving *Herperornis* and the volant *Ichthyornis* from the Niobara Chalk of Western Kansas. *Cretaceous Research*, 19: 225-235.

Chinsamy A, Abdala F. 2008. Palaeobiological implications of the bone microstructure of South American traversodontids (Therapsida: Cynodontia). *South African Journal of Science* 104, 225–230.

Cooper J. 1978. Molt of the black-footed penguin *Spheniscus demersus. International Zoo Yearbook*, 18: 22-27.

Currey JD. 2003. The many adaptations of bone. *Journal of. Biomechanics*. 36, 1487–1495.

Currey JD, Alexander RM. 1985. The thickness of the walls of tubular bones. *Journal of Zoology (London)*, 206: 453-468.

Dacke CG, Arkle S, Cook DJ, Wormstone IM, Jones S, Zaidi M, Bascal ZA. 1993. Medullary bone and avian calcium regulation. *Journal of Experimental Biology*, 184, 63-88.

Domning DP, Buffrénil V. de. 1991. Hydrostasis in the Sirenia: quantitative data and functional interpretations. *Marine Mammal Science*, 7 (4): 331–368.

Dumont ER. 2010. Bone density and the lightweight skeletons of birds. *Proceedings of The Royal Society B Biological Sciences*, 277 1-6.

Fish FE, Stein BR. 1991. Functional correlates of differences in bone density among terrestrial and aquatic genera in the family Mustelidae (Mammalia). *Zoomorphology*, 110: 339-345.

Grémillet D, Dell'Omo G, Ryan PG, Peters G, Ropert-Coudert Y, Weeks SJ. 2004. Offshore diplomacy or how seabirds mitigate intra-specific competition: a case study based on GPS tracking of Cape gannets from neighbouring colonies. *Marine Ecology Progress Series*. Vol. 268: 265–279.

Habib M. 2010. The structural mechanics and evolution of aquaflying birds. *Biological Journal of the Linnean Society*, 99: 687–698.

Habib MB, Ruff CB. 2008. The effects of locomotion on the structural characteristics of avian limb bones. *Zoological Journal of the Linnean Society*, 153: 601-624.

Jarvis MJF. 1972. The systematic position of the South African Gannet. Ostrich 43: 211-215

Kato A, Ropert-Coudert Y, Grémillet D, Cannell B. 2006. Locomotion and foraging strategy in foot-propelled and wing-propelled shallow-diving seabirds. *Marine Ecology Progress Series*. Vol. 308: 293–301.

Kemper J, Roux J-P. 2005. Of squeezers and skippers: Factors determining the age at moult of immature African Penguins *Spheniscus demersus* in Namibia. *Ibis*, 147: 346-352.

Kriloff A, Germain D, Canoville A, Vincent P, Sache M, Laurin M. 2008. Evolution of bone microanatomy of the tetrapod tibia and its use in palaeobiological inference. *Journal of Evolutionary Biology*, 21: 807-826.

de Margerie E, Cubo J, Castanet J. 2002. Bone typology and growth rate: testing and quantifying 'Amprino's rule' in the mallard (*Anas platyrhynchos*). *Comptes Rendus Biologiques*, 325: 221-230.

de Margerie E, Robin J-P, Verrier D, Cubo J, Groscolas R, Castanet J. 2004. Assessing a relationship between bone microstructure and growth rate: a fluorescent labeling study in the king penguin chick (*Aptenodytes patagonicus*). *The Journal of Experimental Biology*, 207: 869-879.

de Margerie E, Sanchez S, Cubo J, Castanet J. 2005. Torsional resistance as a principle component of the structural design of long bones: comparative multivariate evidence in birds. *Anatomical Record*, 282A: 49-66.

Nelson JB. 1978. The Sulidae: Gannets and Boobies. Oxford, *Oxford University Press*.

Padian K, Lamm E-T. 2013. Bone histology of fossil tetrapods- Advaning methods, analysis and interpretation. *University of California Press*.

Ponton F, Elżanowski A, Castanet J, Chinsamy A, de Margerie E, de Ricqlès A, Cubo J. 2004. Variation of the outer circumferential layer in the limb bones of birds. *Acta Ornithologica*, Vol 39: 137-140.

Rand RW. 1959. The biology of guano-producing seabirds. The distribution, abundance and feeding habits of the Cape Gannet, *Morus capensis*, off the south-western coast of the Cape Province. *Investigative Report Sea Fisheries Research Institute*, South Africa. 39: 1-36.

Randall RM, Randall BM. 1981. The annual cycle of the Jackass Penguin *Spheniscus demersus* at St Croix Island, South Africa. In: Cooper J (ed). *Proceedings of the Symposium on birds of the sea and shore*. pp. 427-250.Cape Town: African Seabird Group.

de Ricqlès A, Meunier FJ, Castanet J, Francillon-Vieillot H. 1991. Comparative microstructure of bone. In *Bone, Vol. 3* (ed. Hall BK) pp. 1-78. MA: CRC Press.

de Ricqlès, A, de Buffrenil V. 2001. Bone histology, heterochronies and the return of tetrapods to life in water: where are we? *In* J.M. Mazin and V. de Buffrenil (eds) Secondary Adaptation of Tetrapods to Life in Water. Verlag Dr. Friedrich Pfeil: Munchen. 289-310.

Ropert-Coudert Y, Grémillet D, Ryan PG, Kato A, Naito Y, Le Maho Y. 2004. Between air and water, the plunge dive of the Cape gannet *Morus capensis*. *Ibis*, 146, 281–290.

Schmidt-Nielsen K. 1997. Animal Physiology: Adaptation and Environment. Cambridge & New York: *Cambridge University Press*.

Shubin N, Tabin C, Carroll S. 1997. Fossils, genes and the evolution of animal limbs. *Nature*. Vol 388: 639-648.

Sinclair I, Hockey P, Tarboton W, Ryan P. 2011. Sasol Birds of South Africa. *Struik*. p. 22

Starck JM, Chinsamy A. 2002. Bone microstructure and developmental plasticity in birds and other dinosaurs. *Journal of Morphology*, 254: 232-246.

Vickery J, Brooke M. 1994. The kleptoparasitic interactions between great frigatebirds and masked boobies on Hennderson Island, South Pacific. *Condor*, 96: 331–340.

Wall WP. 1983. The correlation between high limb-bone density and aquatic habits in recent mammals. *Journal of Paleontology*, 57: 197-207.

Whittington P, Klages N, Crawford R, Wolfaardt, A, Kemper J. 2005. Age at first breeding of the African Penguin. *Ostrich*, 76:14-20.

Wilson RP, Wilson M-P T. 1995. The foraging behaviour of the African Penguin *Spheniscus demersus*. *In* Dann P., Norman I. & Reilly P. (eds) The Penguins Surrey Beatty & Sons, Chipping Norton, 244–265.

Additional reading:

Amprino R. 1947. La structure du tissu osseux envisagée comme expression de différences dans la vitesse de l'accroissement. *Archives de Biologie (Liege)*, 58 : 315-330.

Biewener AA, Dial KP. 1995. In vivo strain in the humerus of pigeons (*Columba livia*) during flight. *Journal of Morphology*, 225: 61-75.

de Buffrénil V, Canoville A, D'Anastasio R, Domning DP. 2010. Evolution of sirenian pachyosteosclerosis, a model-case for the study of bone structure in aquatic tetrapods. *Journal of Mammalian Evolution*, 17(2): 101-120.

Canoville A, Laurin M. 2010. Evolution of humeral microanatomy and lifestyle in amniotes, and some comments on paleobiological inferences. *Biological Journal of the Linnean Society*, 100: 384-406.

Castanet J, Currey-Rogers K, Cubo J, Boisard J-J. 2000. Periosteal bone growth rates in extant ratites (ostrich and emu). Implications for assessing growth in dinosaurs. *Comptes Rendus de l'Academie des Sciences. Paris, (Sciences de la Vie),* 323: 543-550.

Chiappe LM. 1995. The first 85 million years of avian evolution. *Nature*, 378: 349–355.

Chinsamy A. 1997. Assessing the biology of fossil vertebrates through bone histology. *Palaeontologia Africana*, 33: 29-35.

Chinsamy-Turan A. 2005. The Microstructure of Dinosaur Bone. *Johns Hopkins University Press*: Baltimore.

Chinsamy A, Elzanowski A, 2001. Evolution of growth pattern in birds. *Nature*, Vol 412: 402-403.

Chinsamy A, Tumarkin-Deratzian A. 2009. Pathologic Bone Tissues in a Turkey Vulture and a Nonavian Dinosaur: Implications for Interpreting Endosteal Bone and Radial Fibrolamellar Bone in Fossil Dinosaurs. *The Anatomical Record*, 292: 1478-1484.

Cook TR, Kato A, Tanaka H, Ropert-Coudert Y, Bost C-A. 2010. Buoyancy under control: Underwater locomotor performance in a deep diving seabird suggests respiratory strategies for reducing foraging effort. *PLoS ONE*, 5(3): e9839.

Crawford RJM, Shelton PA, Cooper J, Brooke RK. 1983. Distribution, population size and conservation of the Cape gannet *Morus capensis*. *South African Journal of Marine Science*, 1:153–174.

Crawford RJM, Williams AJ, Hofmeyr JH, Klages NTW, Randall RM, Cooper J, Dyer BM, Chesselet Y. 1995. Trends of African penguin *Spheniscus demersus* populations in the 20th century. *South African Journal of marine Science,* 16: 101-118.

Crawford RJM, Shannon LJ, Whittington PA. 1999. Population dynamics of the African Penguin *Spheniscus demersus* at Robben Island, South Africa. *Marine Ornithology*, 27: 139-147.

Crawford RJM, Hemming M, Kemper J, Klages NTW, Randall RM, Underhill LG, Venter AD, Ward VL, Wolfaardt AC. 2006. Molt of the African penguin *Spheniscus demersus,* in relation to its breeding season and food availability. *Acta Zoologica Sinica*, 52: 444–447.

Erickson GM, Catanese J, Keaveny TM. 2002. Evolution of the biomechanical material properties of the femur. *Anatomical Record,* 268**:** 115–124.

Feduccia A. 1999. The origin and evolution of birds. New Haven, CT: *Yale University Press.*

Francillon-Vieillot H, Buffrénil V de, Castanet J, Geraudie J, Meunier FJ, Sire JY, Zylberberg L, Ricqlès A de. 1990. Microstructures and mineralization of vertebrate skeletal tissues. *In*: Carter J (ed) Skeletal Biomineralizations: Patterns, Processes and Evolutionary Trends 1. Van Nostrand Reinhold, New York, 471–530.

Germain D, Laurin M. 2005. Microanatomy of the radius and lifestyle in amniotes (Vertebrata, Tetrapoda). *Zoologica Scripta,* 34: 335-350.

Hayashi S, Houssaye A, Nakajima Y, Chiba K, Ando T, et al. 2013. Bone inner structure suggests increasing aquatic adaptations in *Desmostylia* (Mammalia, Afrotheria). *PLoS ONE,* 8(4): e59146.

Jarvis MJF. 1974. The ecological significance of clutch size in the South African Gannet (*Sula capensis* (Lichtenstein)). *Journal of Animal Ecology,* 43: 1-17.

Kemper J, Roux J-P, Bartlett PA, Chesselet Y, James JAC, Jones R, Wepener S, Molloy FJ. 2001. Recent population trends of African Penguins *Spheniscus demersus* in Namibia. *South African Journal of Marine Science*, 23: 429–434.

Kemper J, Roux J-P, Underhill LG. 2008 Effect of age and breeding status on molt phenolology of adult African penguins (*Spheniscus demersus*) in Namibia. *Auk,* 125: 809–819.

Ksepka D, 2007. Thesis. Phylogeny, histology and functional morphology of fossil penguins (Sphenisciformes). Chapter IV. Histological investigations of penguin bone microstructure**.**

Laurin M, Canoville A, Germain D. 2011. Bone microanatomy and lifestyle: A descriptive approach. *Comptes Rendus Palevol*, 10(5): 381-402.

Lovvorn JR. 2001. Upstroke thrust, drag effects, and stroke glide cycles in wingpropelled swimming by birds. *American Zoologist*, 41: 154 -165.

de Margerie E. 2002. Laminar bone as an adaptation to torsional loads in flapping flight. *Journal of Anatomy*, 201: 521-526.

de Margerie E. 2006. Fonction biomécanique des microstructures osseuses chez les oiseaux. *Comptes Rendus Palevol,* 5 : 619-628.

Meister W. 1951. Changes in histological structure of the long bones of birds during the molt. *The Anatomical Record,* Vol.3, no. 1.

Meister W. 1962. Histological structure of the long bones of penguins. *The Anatomical Record*, 143 (4): 377-387.

Middleton KM, Gatesy SM. 2000. Theropod forelimb design and evolution. *Zoological Journal of the Linnean Society,* 28: 149–187.

Padian K, Chiappe LM. 1998. The origin and early evolution of birds. Biological Reviews 73: 1-42.

Padian K, de Ricqlès AJ, Horner JR. 2001. Dinosaurian growth rates and bird origins. *Nature,* 412: 405-408.

Pennycuick C. 2002. Gust soaring as a basis for the flight of petrels and albatrosses (Procellariiformes). *Avian Science,* 2: 1–12.

Shelton PA, Crawford RJM, Cooper J, Brooke RK. 1984. Distribution, population size and conservation of the jackass penguin *Spheniscus demersus*, *South African Journal of Marine Science*, 2:1, 217-257.

Simons ERL. 2009. Thesis. The evolution of forelimb morphology and flight mode in extant birds. Chapter 4: Bone microstructure, primary vascular canal orientation and flight mode in birds.

Simons ELR, Hieronymus TL, O'Connor PM. 2011. Cross sectional geometry of the forelimb skeleton and flight mode in pelecaniform birds. *Journal of Morphology*, 272: 958-971.

Straehl FR, Scheyer TM, Forasiepi AM, MacPhee RD, Sa´nchez-Villagra MR. 2013. Evolutionary patterns of bone histology and bone compactness in Xenarthran mammal long bones. *PLoS ONE*, 8(7): e69275.

Swartz SM, Bennett MB, Carrier DR. 1992. Wing bone stresses in free flying bats and the evolution of skeletal design for flight. *Nature*, 359: 726-729.

Taylor MA. 1994. Stone, bone or blubber? Buoyancy control strategies in aquatic tetrapods. *In* : *Mechanics and physiology of animals swimming*, Maddock L, Bone Q, Rayner JMV (Eds). Cambridge: Cambridge University Press. 151–161.

Taylor MA. 2000. Functional significance of bone ballastin in the evolution of buoyancy control strategies by aquatic tetrapods. *Historical Biology*, 14(1-2): 15-31.

Du Toit M, Boere GC, Cooper J, de Villiers MS, Kemper J, Lenten B, Petersen SL, Simmons RE, Underhill LG, Whittington PA, Byers O (eds). 2003. Conservation assessment and management plan for Southern African seabirds. Cape Town: Avian Demography Unit & Apple Valley: IUCN/SSC Conservation Breeding Specialist Group.

Watanuki Y, Wanless S, Harris M, Lovvorn JR, Miyazaki M, Tanaka H, Sato K. 2006. Swim speed and stroke patterns in wing-propelled divers: a comparison among alcids and a penguin. *Journal of Experimental Biology*, 209: 1217-1230.

Wilson LE. 2012. Thesis. Paleobiology of Hesperornithiforms (Aves) from the Campanian Western interior seaway of North America, with analyses of extant penguin bone histology.

APPENDIX

Table A1: The complete data relevant to the biological samples (Compiled by Dr. Nola Parsons, SANCCOB). Note: The head length was measured for the penguins and the beak length (mm) was measured for the gannets.

Species	Bird N°	Date admit	Area from	Date died	Age	Gender	Head length (mm)	Weight (kg)	Condition	Cause of Death (PTS = Put to sleep / DOA = Dead on arrival)
African penguin	**064**	19.2.12	Boulders	24.2.12	Hatchling	Male	91.1	1.25	Moderate	PST - Fractured leg
	466	5.12.11	Betty's Bay	3.4.12	juvenile	Female	115.8	2.40	Good	PTS-Poor feather+bumble foot
	116	2.4.12	Boulders	2.4.12	juvenile	Male	121.7	2.00	Poor	PTS - Fractured beak
	241	30.7.12	Robben Is.	1.8.12	juvenile	Male	108.1	1.40	Poor	Died - Weak, thin, enteritis
	146	25.4.12	Kalk Bay	25.4.12	Adult	Male	121.9	2.38	Good	DOA - Wounds + peritonitis
	191	20.6.12	Boulders	19.6.12	Adult	Male	127.2	2.80	Good	DOA - Ruptured intestine
	192	20.6.12	Boulders	19.6.12	Adult	Male	127.7	3.00	Good	DOA - Blood loss (trauma)
	167	23.5.12	Betty's Bay	23.5.12	Adult	Female	115.5	2.56	Good	PTS - leg + abdominal wounds
	231	20.7.12	Betty's Bay	20.7.12	Adult	Female	112.4	2.42	Good	PST - Fractured leg
	524	19.9.12	Betty's Bay	19.9.12	Adult	Female	118.1	3.55	Fat	PST - Fractured leg
Cape gannet	**G04**	27.2.12	Muizenberg	27.2.12	juvenile	Male	92.8	1.60	Poor	PTS - Fractured wing
	G17	2.4.12	Muizenberg	2.4.12	juvenile	Female	90.8	1.38	Poor	PTS - Fractured wing
	G19	5.4.12	Fishhoek	10.4.12	juvenile	Male	91.8	1.78	Moderate	PTS - Fractured wing
	G20	10.4.12	Robben Is.	12.4.12	juvenile	Female	87.7	1.38	Poor	Died - Necrotic eneritis
	G59	1.9.12	Llandudno	1.9.12	Adult	Male	83.4	2.25	Good	PTS - Fractured wing
	G61	27.9.12	Fish hoek	18.9.12	Adult	Male	91.4	2.10	Thin	H
	G24	25.4.12	Muizenberg	8.5.12	Adult	Female	89.3	2.20	Good	PTS - not standing
	G56	21.5.12	Fishhoek	21.5.12	Adult	Female	78.8	1.90	Thin	DOA - perforated intestine
	G57	21.5.12	Fishhoek	21.5.12	Adult	Female	88.8	1.55	Emaciated	Died - Emaciation

Table A2: Measurements of the fore-limb bones of *Spheniscus demersus* and *Morus capensis* as shown on Figure 3 (Materials and Methods). Some bones have not been sampled because they were broken. All measurements are in millimeters (mm). [Abbreviations: BL: Bone length; PW: Proximal width; DW: Distal width; MSD: Mid-shaft diameter].

Bird N°	Humerus				Radius				Ulna				Carpometacarpus			
	BL	PW	DW	MSD	BL	PW	DW	MSD	BL	PW	DW	MSD	BL	PW	DW	MSD
064	59.68	11.99	12.35	10.95	33.84	6.74	6.43	8.13	37.86	6.36	7.40	8.61	-	-	-	
466	65.12	17.39	16.43	10.27	47.42	7.54	8.17	10.03	45.54	7.95	7.79	11.97	36.56	11.82	12.33	12.33
116	75.67	21.81	16.83	13.58	50.36	8.51	8.74	12.09	52.96	8.65	8.04	16.27	44.42	14.62	15.13	15.67
241	68.28	20.63	16.26	12.79	47.82	9.09	7.65	10.81	49.46	7.88	8.46	12.79	41.06	14.94	14.26	13.03
146	69.54	18.26	15.94	12.95	47.23	8.04	7.68	11.43	49.21	8.26	8.35	13.54	41.02	13.42	15.02	14.88
191	70.95	20.34	16.38	14.21	49.87	8.05	8.98	10.57	50.79	7.54	8.56	13.78	-	-	-	-
192	72.73	21.42	25.01	13.98	49.87	8.66	8.81	12.35	52.22	8.73	8.92	14.59	42.03	13.88	16.26	15.45
167	67.68	16.19	21.47	11.69	48.33	8.31	8.66	10.59	48.48	7.35	8.37	13.39	39.53	13.60	14.94	14.10
231	70.10	20.90	16.42	12.73	45.52	7.89	8.43	10.55	47.53	7.32	7.29	12.77	40.06	13.38	15.54	13.44
524	63.44	17.74	16.09	12.13	47.51	7.64	8.27	11.34	44.78	9.44	7.59	11.94	37.20	12.62	14.10	14.34
G04	221.15	29.15	22.89	10.07	190.25	7.67	11.99	5.62	195.74	16.49	15.96	8.38	93.22	19.04	13.02	6.28
G17	207.97	27.62	22.36	10.49	185.76	7.82	15.30	5.73	185.29	16.31	16.13	8.02	91.36	12.31	13.54	7.37
G19	217.37	27.77	21.26	9.07	185.54	7.99	13.66	5.57	190.71	15.71	16.30	8.13	90.26	18.55	12.98	6.59
G20	216.55	27.55	21.96	9.79	186.76	8.21	14.77	5.08	190.36	16.79	16.56	7.56	88.36	18.73	12.14	5.69
G59	212.53	27.28	20.89	10.57	179.92	7.17	11.26	5.04	183.18	15.23	16.07	8.24	85.76	17.94	14.19	6.81
G61	224.60	29.47	22.77	10.87	190.09	7.93	11.84	5.85	202.75	16.86	16.62	8.89	88.26	18.98	12.88	6.93
G24	223.39	27.34	22.24	11.28	191.99	8.57	13.68	5.15	197.36	16.17	15.44	7.69	91.89	18.95	14.54	6.56
G56	198.4	29.32	22.07	10.47	170.55	8.32	11.92	5.44	173.19	15.83	16.41	8.08	79.91	17.79	11.67	6.59
G57	208.24	29.11	22.41	10.73	181.16	7.98	12.27	5.51	185.77	15.98	17.61	7.89	87.18	18.58	13.83	7.09

Table A3: Measurements of the hind limb bones of *Spheniscus demersus* and *Morus capensis* as shown on Figure 3 (Materials and Methods). Some bones have not been sampled because they were broken. All measurements are in millimeters (mm). [Abbreviations: BL: Bone length; PW: Proximal width; DW: Distal width; MSD: Mid-shaft diameter].

Bird N°	Femur				Tibiotarsus				Tarsometatarsus				Phalanx			
	BL	PW	DW	MSD	BL	PW	DW	MSD	BL	PW	DW	MSD	BL	PW	DW	MSD
064	67.78	14.48	12.99	7.08	87.96	16.73	13.88	7.09	31.27	15.87	16.79	14.25	-	-	-	-
466	67.74	14.71	14.18	7.42	98.49	17.88	13.61	6.62	29.83	16.03	18.90	14.84	-	-	-	-
116	76.57	17.19	16.07	7.61	117.28	17.67	14.09	7.63	35.16	16.26	20.44	15.67	25.38	10.09	6.91	5.94
241	71.52	15.66	16.68	7.90	103.18	18.92	14.60	6.88	32.89	16.31	19.76	15.23	-	-	-	-
146	74.95	15.88	16.53	7.64	109.34	17.36	13.99	7.66	33.42	15.09	20.28	15.94	23.01	8.72	6.58	6.13
191	-	-	-	-	111.69	21.62	14.43	7.33	34.57	15.27	20.26	15.25	-	-	-	-
192	-	-	-	-	112.25	21.82	14.52	8.81	34.55	17.36	20.47	15.93	-	-	-	-
167	71.66	16.24	13.97	7.18	103.02	21.24	13.24	6.11	33.25	14.41	19.69	17.65	-	-	-	-
231	-	-	-	-	103.68	18.10	13.44	6.64	31.85	14.87	19.68	13.91	-	-	-	-
524	61.21	14.45	14.02	6.86	99.25	17.16	14.66	6.98	30.04	15.24	18.91	14.28	-	-	-	-
G04	73.04	15.67	15.93	6.87	107.69	20.76	14.12	7.23	62.04	15.02	16.92	8.92	-	-	-	-
G17	70.22	15.09	14.81	6.58	104.07	18.75	13.76	7.26	59.78	14.36	17.64	8.16	-	-	-	-
G19	71.82	13.97	16.73	6.97	108.94	16.55	13.18	7.65	62.97	14.03	16.79	8.28	-	-	-	-
G20	72.05	14.65	16.80	7.42	107.11	18.13	14.09	7.38	59.43	14.68	16.81	8.34	-	-	-	-
G59	69.81	13.92	15.36	6.58	103.41	20.37	12.74	7.76	57.04	14.73	16.64	8.20	-	-	-	-
G61	72.58	15.56	16.93	7.91	109.37	19.18	14.58	7.85	59.85	14.69	18.03	8.52	-	-	-	-
G24	72.42	14.61	16.74	7.71	105.69	18.82	15.22	7.93	61.15	14.08	17.41	8.23	-	-	-	-
G56	69.29	13.29	15.77	8.32	100.63	16.43	13.49	8.13	56.83	14.01	17.09	8.68	-	-	-	-
G57	69.03	14.13	15.96	7.32	103.84	19.65	12.35	7.43	58.50	13.51	18.02	8.57	-	-	-	-

Table A4: Measurements and calculation of the average diameter of the whole bone cross-section (at the midshaft level) and the average diameter of the medullary cavity as described in Figure 5 in the Material and methods section in order to calculate the *k* parameter. All measurements are in millimeters (mm). [Abbreviations: B: Bone; Sd: Section diameter; MCd: Medullary cavity diameter; Avg Sd: average section diameter; Avg MCd: average medullary cavity diameter; Ca: Carpometacarpus; Fe: Femur; Hu: Humerus; Phalanx: Px; Radius: Ra; Ta: Tarsometatarsus; Ti: Tibiotarsus; Ul: Ulna].

	B	Sd 1	MCd 1	Sd 2	MCd 2	Sd 3	MCd 3	Avg Sd	Avg MCd	B	Sd 1	MCd 1	Sd 2	MCd 2	Sd 3	MCd 3	Avg Sd	Avg MCd
064	**Fe**	6.33	2.25	6.13	2.05	5.57	2.07	6.01	2.12	**Ta**	12.78	3.54	3.84	1.18	4.32	0.92	6.98	1.88
	Hu	10.53	0.20	3.53	0.64	7.18	0.00	7.08	0.28	**Ti**	7.24	0.52	5.72	0.49	7.10	0.56	6.69	0.52
	Ra	7.22	0.00	2.62	0.10	4.50	0.00	4.78	0.03	**Ul**	7.70	1.92	2.86	1.02	5.29	2.14	5.28	1.69
466	**Ca**	8.12	4.22	2.91	0.58	5.55	1.49	5.53	2.10	**Ta**	5.33	2.23	10.53	3.53	3.44	1.42	6.43	2.39
	Fe	12.32	4.93	10.99	4.67	12.30	5.33	11.87	4.98	**Ti**	6.82	2.58	6.33	3.08	6.11	2.22	6.42	2.62
	Hu	9.25	2.74	6.90	0.99	4.85	0.83	7.00	1.52	**Ul**	11.13	0.00	7.68	1.49	2.80	0.00	7.20	0.50
	Ra	9.00	2.53	3.31	0.86	5.34	1.30	5.88	1.57									
116	**Ca**	9.99	1.45	1.94	0.00	5.33	0.00	5.75	0.48	**Ra**	11.65	0.00	3.47	0.09	5.76	0.00	6.96	0.03
	Fe	7.67	2.73	7.56	2.69	7.43	2.38	7.56	2.60	**Ta**	4.59	0.90	5.53	1.63	1.30	0.00	3.81	0.84
	Hu	13.77	0.00	4.55	0.00	10.09	0.46	9.47	0.15	**Ti**	7.30	2.39	7.01	2.15	6.44	2.45	6.92	2.33
	Px	5.30	3.81	5.57	3.67	4.59	1.02	5.15	2.83	**Ul**	15.23	0.00	3.36	0.00	11.29	0.38	9.96	0.13
241	**Ca**	16.50	5.14	3.36	0.61	6.54	1.70	8.80	2.49	**Ta**	4.15	1.52	3.68	1.61	3.94	0.00	3.92	1.04
	Fe	12.74	3.85	10.59	3.58	11.91	4.37	11.75	3.93	**Ti**	6.38	1.86	5.30	0.00	6.02	2.57	5.90	1.48
	Hu	12.20	3.29	4.50	0.00	7.35	0.00	8.02	1.10	**Ul**	10.10	4.91	2.99	0.75	6.24	0.00	6.45	1.89
	Ra	16.61	4.83	4.95	1.12	6.41	1.60	9.32	2.52									
146	**Ca**	9.39	5.40	2.82	0.57	5.95	0.83	6.06	2.27	**Ra**	10.83	5.35	3.23	0.75	6.23	0.75	6.76	2.28
	Fe	7.51	2.71	6.69	2.63	7.30	3.23	7.17	2.86	**Ta**	4.27	2.62	4.01	1.98	3.76	1.61	4.01	2.07
	Hu	12.17	2.66	3.66	0.00	7.58	0.98	7.80	1.21	**Ti**	8.20	4.37	6.74	4.02	7.24	3.97	7.39	4.12
	Px	6.98	6.09	6.02	5.50	4.77	2.50	5.92	4.70	**Ul**	13.13	5.36	3.35	0.82	5.41	0.90	7.30	2.36
191	**Hu**	15.47	6.42	7.22	1.49	9.11	1.48	10.60	3.13	**Ti**	6.38	2.86	6.91	2.84	6.04	2.50	6.44	2.73
	Ra	9.87	1.98	3.19	0.61	5.02	0.00	6.03	0.86	**Ul**	12.56	0.00	3.12	0.48	7.40	0.00	7.69	0.16
	Ta	3.71	1.10	2.11	0.00	4.98	0.00	3.60	0.37									
192	**Ca**	9.45	0.37	3.00	0.00	5.60	0.00	6.02	0.12	**Ta**	6.15	3.84	14.64	10.11	7.25	2.58	9.35	5.51
	Hu	11.42	4.56	5.15	1.00	7.11	1.32	7.89	2.29	**Ti**	11.77	5.73	10.74	4.47	11.79	5.52	11.43	5.24
	Ra	15.68	4.37	5.38	0.30	7.81	0.85	9.62	1.84	**Ul**	16.53	6.21	4.31	0.33	8.83	0.88	9.89	2.47
167	**Ca**	3.41	1.12	5.79	1.90	5.40	1.26	4.87	1.43	**Ta**	13.90	2.71	13.99	10.49	5.33	3.52	11.08	5.57
	Fe	11.52	4.71	11.29	4.82	11.42	5.14	11.41	4.89	**Ti**	6.41	2.97	5.69	2.60	6.53	2.74	6.21	2.77
	Hu	16.61	3.32	6.63	0.74	10.35	0.97	11.20	1.67	**Ul**	11.98	4.37	3.28	0.62	6.31	0.49	7.19	1.83
	Ra	9.45	4.10	3.24	0.66	6.01	1.47	6.24	2.08									

Continued…

	B	Sd 1	MCd 1	Sd 2	MCd 2	Sd 3	MCd 3	Avg Sd	Avg MCd	B	Sd 1	MCd 1	Sd 2	MCd 2	Sd 3	MCd 3	Avg Sd	Avg MCd
231	**Ca**	16.30	7.47	3.39	0.49	5.79	1.21	8.49	3.06	**Ta**	17.50	5.84	7.25	2.80	9.68	4.54	11.48	4.39
	Hu	11.00	4.28	8.33	1.84	4.84	1.05	8.06	2.39	**Ti**	8.40	3.80	8.10	3.63	8.68	4.19	8.39	3.87
	Ra	10.38	2.49	5.95	0.00	3.01	0.50	6.45	1.00	**Ul**	11.75	0.00	5.85	0.00	3.04	0.78	6.88	0.26
524	**Ca**	8.21	3.14	3.10	0.49	5.08	2.18	5.46	1.94	**Ta**	14.85	4.39	4.91	1.90	3.30	0.88	7.68	2.39
	Fe	7.90	3.77	6.68	3.06	7.64	3.49	7.41	3.44	**Ti**	6.65	2.60	6.86	2.90	6.29	2.78	6.60	2.76
	Hu	10.81	2.64	6.36	0.00	4.67	0.00	7.28	0.88	**Ul**	17.93	5.65	10.22	1.72	5.38	0.89	11.18	2.75
	Ra	17.37	8.71	5.99	0.75	7.42	1.05	10.26	3.51									
G04	**Hu**	8.69	6.32	9.19	6.68	9.68	7.99	9.19	7.00	**Fe**	6.72	5.36	7.12	5.59	7.51	5.95	7.12	5.63
	Ra	4.84	3.46	5.33	3.82	5.05	3.63	5.07	3.63	**Ti**	6.61	4.81	5.23	3.60	7.21	5.11	6.35	4.50
	Ul	7.76	5.83	7.67	6.30	7.98	6.16	7.80	6.10	**Ta**	8.05	6.50	4.49	3.04	7.56	5.44	6.70	4.99
	Ca	6.12	4.39	5.70	4.18	5.23	4.89	5.68	4.49									
G17	**Hu**	13.23	10.31	10.74	7.35	10.94	7.74	11.64	8.47	**Fe**	10.37	7.73	10.21	7.77	9.36	7.21	9.98	7.57
	Ra	4.56	3.50	3.88	2.62	4.79	3.52	4.41	3.21	**Ti**	10.36	7.86	7.87	5.60	8.08	5.53	8.77	6.33
	Ul	6.11	4.22	7.40	5.62	7.37	5.51	6.96	5.12	**Ta**	15.15	11.70	12.25	7.53	7.84	4.51	11.75	7.92
	Ca	10.23	7.20	9.50	7.29	8.59	6.82	9.44	7.10									
G19	**Hu**	8.21	5.72	9.32	7.52	9.93	8.29	9.15	7.18	**Fe**	11.49	9.04	10.95	8.58	10.86	8.08	11.10	8.57
	Ra	4.80	3.53	4.99	3.68	4.71	3.56	4.83	3.59	**Ti**	13.18	10.13	9.30	6.27	11.70	8.43	11.39	8.27
	Ul	11.36	9.00	11.05	8.90	10.91	9.10	11.11	9.00	**Ta**	8.07	6.22	6.07	4.09	3.62	1.82	5.92	4.04
	Ca	8.45	7.01	10.07	7.53	9.80	7.27	9.44	7.27									
G20	**Hu**	9.80	7.72	8.26	5.46	9.60	6.80	9.22	6.66	**Fe**	6.49	4.96	7.19	5.53	6.78	4.84	6.82	5.11
	Ra	4.81	3.63	4.90	3.65	4.90	3.71	4.87	3.66	**Ti**	7.32	5.80	5.98	3.91	5.46	3.64	6.26	4.45
	Ul	7.39	5.86	7.71	5.80	7.53	5.72	7.55	5.79	**Ta**	8.15	6.67	3.28	1.96	8.20	6.32	6.54	4.98
	Ca	5.33	4.24	6.10	4.07	6.22	4.41	5.88	4.24									
G59	**Hu**	13.04	10.53	11.56	7.93	10.63	6.60	11.74	8.35	**Fe**	7.18	5.47	5.94	4.60	6.36	4.90	6.49	4.99
	Ra	4.86	3.51	5.01	3.54	4.79	3.62	4.89	3.56	**Ti**	6.85	5.43	5.82	4.59	5.19	3.94	5.96	4.65
	Ul	10.95	8.50	10.58	7.95	10.66	8.36	10.73	8.27	**Ta**	7.68	3.96	7.44	5.93	3.37	2.04	6.16	3.98
	Ca	6.14	4.41	5.87	4.20	5.15	4.18	5.72	4.26									
G61	**Hu**	8.61	6.07	10.42	8.66	9.89	7.32	9.64	7.35	**Fe**	7.33	5.97	7.39	5.79	7.03	5.79	7.25	5.85
	Ra	4.96	3.78	5.47	4.03	5.25	3.91	5.23	3.91	**Ti**	9.97	6.75	7.02	5.81	6.19	5.08	7.73	5.88
	Ul	8.13	6.64	8.04	6.52	7.95	6.62	8.04	6.59	**Ta**	8.03	7.09	7.56	4.70	3.28	2.14	6.29	4.64
	Ca	5.82	4.86	6.65	4.88	6.00	4.84	6.16	4.86									
G24	**Hu**	13.14	9.10	13.20	10.16	10.78	7.12	12.37	8.79	**Fe**	9.73	7.50	10.51	8.29	9.94	7.84	10.06	7.88
	Ra	5.07	3.66	4.55	3.27	4.86	3.39	4.83	3.44	**Ti**	9.62	7.47	8.07	6.00	7.35	5.42	8.35	6.30
	Ul	12.25	9.22	11.24	8.97	11.33	8.64	11.61	8.94	**Ta**	7.79	6.45	4.62	2.97	7.46	5.70	6.62	5.04
	Ca	10.21	7.10	7.85	6.25	10.24	7.20	9.44	6.85									

Continued…

	B	Sd 1	MCd 1	Sd 2	MCd 2	Sd 3	MCd 3	Avg Sd	Avg MCd	B	Sd 1	MCd 1	Sd 2	MCd 2	Sd 3	MCd 3	Avg Sd	Avg MCd
G56	Hu	10.51	8.56	8.60	5.96	9.52	7.37	9.54	7.30	Fe	7.71	6.27	6.93	5.54	6.71	5.57	7.12	5.80
	Ra	5.28	3.76	5.21	3.94	5.27	3.87	5.25	3.86	Ti	11.31	8.76	9.87	7.72	8.21	6.28	9.80	7.59
	Ul	8.06	6.14	7.94	6.30	7.55	5.35	7.85	5.93	Ta	8.15	6.74	7.53	5.10	4.25	3.18	6.64	5.01
	Ca	8.43	6.08	8.37	6.04	7.91	6.20	8.24	6.11									
G57	Hu	14.47	11.18	12.54	8.33	11.43	6.99	12.82	8.83	Fe	9.25	6.87	10.18	7.57	10.07	7.73	9.83	7.39
	Ra	5.04	3.48	5.12	3.28	4.99	3.22	5.05	3.33	Ti	7.40	5.55	4.98	3.47	5.15	3.69	5.84	4.23
	Ul	9.92	7.47	10.41	7.06	10.18	7.12	10.17	7.22	Ta	8.53	6.84	7.64	4.43	3.25	2.02	6.47	4.43
	Ca	8.61	5.54	8.32	5.40	6.79	5.14	7.91	5.36									

Table A5: Values for the *k* index (Currey and Alexander, 1985) for all the African penguin and Cape gannet bones. (AF: African penguin; CG: Cape gannet).

Age	Species	No	Gender	Humerus	Radius	Ulna	Carpo-metacarpus	Femur	Tibio-tarsus	Tarso-metatarsus
Hatchling	**AF**	**064**	**Male**	0.04	0.01	0.32	-	0.35	0.08	0.27
Juvenile	**AF**	**466**	**Female**	0.22	0.27	0.07	0.38	0.42	0.41	0.37
Juvenile	**AF**	**116**	**Male**	0.02	0.00	0.01	0.08	0.34	0.34	0.22
Juvenile	**AF**	**241**	**Male**	0.14	0.27	0.29	0.28	0.33	0.25	0.27
Adult	**AF**	**146**	**Male**	0.16	0.34	0.32	0.37	0.40	0.56	0.52
Adult	**AF**	**191**	**Male**	0.30	0.14	0.02	-	-	0.42	0.10
Adult	**AF**	**192**	**Male**	0.29	0.19	0.25	0.02	-	0.46	0.59
Adult	**AF**	**167**	**Female**	0.15	0.33	0.25	0.29	0.43	0.45	0.50
Adult	**AF**	**231**	**Female**	0.30	0.15	0.04	0.36	-	0.46	0.38
Adult	**AF**	**524**	**Female**	0.12	0.34	0.25	0.35	0.46	0.42	0.31
Juvenile	**CG**	**G04**	**Male**	0.76	0.72	0.78	0.79	0.79	0.71	0.75
Juvenile	**CG**	**G17**	**Female**	0.73	0.73	0.74	0.75	0.76	0.72	0.67
Juvenile	**CG**	**G19**	**Male**	0.78	0.74	0.81	0.77	0.77	0.73	0.68
Juvenile	**CG**	**G20**	**Female**	0.72	0.75	0.77	0.72	0.75	0.71	0.76
Adult	**CG**	**G59**	**Male**	0.71	0.73	0.77	0.75	0.77	0.78	0.65
Adult	**CG**	**G61**	**Male**	0.76	0.75	0.82	0.79	0.81	0.76	0.74
Adult	**CG**	**G24**	**Female**	0.71	0.71	0.77	0.73	0.78	0.75	0.76
Adult	**CG**	**G56**	**Female**	0.76	0.73	0.76	0.74	0.81	0.77	0.75
Adult	**CG**	**G57**	**Female**	0.69	0.66	0.71	0.68	0.75	0.72	0.68

Table A6: Complete bone histological description for the African penguin (*Spheniscus demersus*) observed under normal and polarized light at ×40, ×100 and ×400 magnification. [Abbreviations: B: Bone; OCL: Outer circumferential layer; ICL: Inner circumferential layer; a: absent; p: present; pp: present in some regions; c: circumferential; l:longitudinal; r: radial; o: reticular; po: primary osteons; so: secondary osteons; rc: resorption cavities; svc: simple vascular canals; wbm: woven bone matrix; lb: lamellar bone; Ca: Carpometacarpus; Fe: Femur; Hu: Humerus; Px: Phalanx; Ra: Radius; Ta: Tarsometatarsus; Ti: Tibiotarsus; Ul: Ulna].

Bird No	B	OCL	OCL thickness	ICL	ICL thickness	Mid-cortical layer- Type of vascularization	Mid-cortical layer - Type of osteons	Mid-cortical layer- Type of bone tissue
064	**Hu**	a	-	a	-	r,l	po ,svc	wbm
064	**Ra**	a	-	a	-	r,l	po,svc	wbm
064	**Ul**	a	-	a	-	l	po,svc	wbm
064	**Fe**	a	-	a	-	r,l	po,svc	wbm
064	**Ti**	a	-	a	-	r,l	po,svc	wbm
064	**Ta**	a	-	a	-	r,l	po,svc	wbm
466	**Hu**	pp	thin	pp	thin	l,o,r	po,so,svc	wbm
466	**Ra**	pp	thin	a	-	l,o,r	po,svc	wbm
466	**Ul**	pp		pp		l,o,r	po,few svc	wbm
466	**Ca**	pp	thin	pp	thin	l,o	po,few so,few svc	wbm
466	**Fe**	a	-	pp	thin	l,o	po,few svc	wbm
466	**Ti**	a	-	pp	thin	l,o	po,few svc	wbm
466	**Ta**	a	-	pp	thin	l,o	po,few svc	wbm
116	**Hu**	a	-	a	-	c,l,o	po,few so	wbm, few lb
116	**Ra**	pp	thin	a	-	l,o,r	po,few so,few svc	wbm, few lb
116	**Ul**	a	-	a	-	c,l,r	few po,few svc	wbm
116	**Ca**	a	-	pp	thin	l,o	few po,few so,svc	wbm, few lb
116	**Fe**	a	-	a	-	l,o,r	po, few rc	wbm
116	**Ti**	a	-	a	-	l,o	few po,so,few rc, svc	wbm, few lb
116	**Ta**	a	-	pp	thin	l	few po,so,few rc, hc	wbm
116	**Px**	a	-	a	-	l	po,svc	wbm
241	**Hu**	a	-	pp	thin	l,o,r	po,svc	wbm
241	**Ra**	a	-	a	thin	r	po,svc	wbm, few lb
241	**Ul**	a	-	a	-	l,o	few po,svc	wbm, few lb
241	**Ca**	a	-	a	-	l,o	few po,svc	wbm
241	**Fe**	a	-	a	thin	r,l	po,svc	wbm
241	**Ti**	a	-	pp	thin	l,o,r	po,few svc	wbm
241	**Ta**	a	-	pp	thin	l	po,svc	wbm, few lb
146	**Hu**	a	-	a	-	l,o,r	po,so,rc	wbm, few lb
146	**Ra**	a	-	pp	thin	l,o	po,so,rc	wbm, few lb
146	**Ul**	a	-	pp	thick	l,o,r	po,so	wbm
146	**Ca**	a	-	pp	thin	l,o	po,rc	wbm

Continued…								
146	**Fe**	p	thin	p	thin	c,l,o	few po,so,rc	wbm, few lb
146	**Ti**	pp	thin	p	thick	l,o	po,so,rc	wbm
146	**Ta**	a	-	a	-	c,l,o	po,so,rc, svc	wbm
146	**Px**	a	-	a	-	o	po,rc	wbm
191	**Hu**	pp	thin	p	thin	l,o,r	svc,po,so,few rc	wbm
191	**Ra**	pp	thin	pp	thin	l,o	po,so,rc	wbm
191	**Ul**	a	-	a	-	l,o	po,so	wbm
191	**Ti**	p	thin	p	thick	l,o,r	po,svc	wbm
191	**Ta**	pp	thin	pp	thin	l	po,so,rc, svc	wbm, few lb
192	**Hu**	p	thin	pp	thin	l,o	po,few so,few rc	wbm
192	**Ra**	pp	thin	pp	thin	l,o	po,so,rc, few svc	wbm, few lb
192	**Ul**	p	thin	a	-	l,o	po,so,rc, few svc	wbm, few lb
192	**Ca**	pp	thin	a	-	l,o	po,so	wbm
192	**Ti**	p	thin	p	thin	o	po,svc	wbm
192	**Ta**	pp	thin	pp	thin	l,o	po,svc	wbm
167	**Hu**	a	-	a	-	o	po,few so	wbm, few lb
167	**Ra**	pp	thin	pp	thin	l	po,so	wbm
167	**Ul**	a	-	pp	thin	l	po	wbm, few lb
167	**Ca**	pp	thin	p	thin	l,o,r	po,so	wbm
167	**Fe**	p	thin	p	thick	l,o	po,few so	wbm, few lb
167	**Ti**	p	thin	p	thick	l,o,r	po,few so	wbm
167	**Ta**	pp	thin	p	thick	l,o	po,so	wbm
231	**Hu**	pp	thin	pp	thick	l,o	po	wbm
231	**Ra**	a	-	pp	thick	l,o	po	wbm
231	**Ul**	pp	thin	pp	thick	l,o	po,svc	wbm
231	**Ca**	p	thin	p	thick	l,o	po,so	wbm, few lb
231	**Ti**	p	thin	p	thick	l,o	po,few so	wbm
231	**Ta**	pp	thin	a	-	l	po	wbm
524	**Hu**	pp	thin	pp	thick	l,o	po	wbm, few lb
524	**Ra**	pp	thin	pp	thick	l,o	po	wbm, few lb
524	**Ul**	pp	thin	pp	thick	l,o	po,so	wbm
524	**Ca**	p	thin	p	thin	l,o	po,so	wbm
524	**Fe**	p	thick	p	thin	l,o	po,so	wbm, few lb
524	**Ti**	p	thin	p	thick	l,o,r	po,few so	wbm
524	**Ta**	pp	thin	pp	thick	l,o	few po,svc	wbm

Table A7: Complete bone histological description for the Cape gannet (*Morus capensis*) observed under normal and polarized light at ×40, ×100 and ×400 magnification. Abbreviations: B: Bone; OCL: Outer circumferential layer; ICL: Inner circumferential layer; a: absent; p: present; pp: present in some regions; c: circumferential; l:longitudinal; r: radial; o: reticular; po: primary osteons; so: secondary osteons; rc: resorption cavities; wbm: woven bone matrix; lb: lamellar bone; Ca: Carpometacarpus; Fe: Femur; Hu: Humerus; Phalanx: Px; Radius: Ra; Ta: Tarsometatarsus; Ti: Tibiotarsus; Ul: Ulna].

Bird No	B	OCL	OCL thickness	ICL	ICL thickness	Mid-cortical layer-Type of vascularization	Mid-cortical layer-Type of osteons	Mid-cortical layer-Type of bone tissue
G04	**Hu**	pp	thin	a	-	l,o	po	wbm
G04	**Ra**	pp	thin	a	-	l,o	po	wbm
G04	**Ul**	pp	thin	a	-	l,o	po	wbm
G04	**Ca**	pp	thin	a	-	l,o	po	wbm
G04	**Fe**	p	thin	p	thin	l,o	po	wbm
G04	**Ti**	p	thin	a	-	l,o	po	wbm, few lb
G04	**Ta**	p	thin	p	thin	l,o,r	po,few so,few rc	wbm
G17	**Hu**	p	thin	pp	thin	o	po	wbm
G17	**Ra**	p	thin	pp	thin	l	po	wbm
G17	**Ul**	p	thick	pp	thin	l,o	po	wbm
G17	**Ca**	p	thin	pp	thin	l,o	po	wbm
G17	**Fe**	p	thin	p	thin	l,o	po	wbm
G17	**Ti**	p	thin	pp	thin	l	po	wbm
G17	**Ta**	p	thin	pp	thin	o	po,few so,few rc	wbm
G19	**Hu**	p	thin	p	thin	l,o	po	wbm
G19	**Ra**	p	thin	p	thin	l	po	wbm
G19	**Ul**	p	thin	p	thin	o	po	wbm
G19	**Ca**	p	thin	p	thin	o	po	wbm
G19	**Fe**	p	thick	p	thin	o	po	wbm
G19	**Ti**	p	thin	pp	thin	l,o,r	po	wbm, few lb
G19	**Ta**	p	thin	p	thick	l,o	po,few so,few rc	wbm, few lb
G20	**Hu**	p	thin	pp	thin	o	po	wbm
G20	**Ra**	p	thin	a	-	o	po	wbm
G20	**Ul**	p	thin	pp	thin	l	po	wbm
G20	**Ca**	pp	thin	pp	thin	o	po	wbm
G20	**Fe**	p	thick	p	thick	o	po	wbm
G20	**Ti**	p	thin	p	thin	l	po	wbm
G20	**Ta**	p	thin	p	thick	o	po,few so	wbm
G59	**Hu**	p	thin	p	thick	c,l,o	po,few rc	wbm
G59	**Ra**	p	thick	p	thick	l	po	wbm
G59	**Ul**	p	thick	p	thick	c,l	po	wbm
G59	**Ca**	p	thick	p	thick	l	po	wbm

Continued…								
G59	**Fe**	p	thin	p	thick	c,l	po	wbm
G59	**Ti**	p	thin	p	thick	o	po	wbm
G59	**Ta**	p	thin	p	thin	l	po,few so,few rc	wbm
G61	**Hu**	p	thick	p	thick	c,l,o	po	wbm
G61	**Ra**	p	thin	p	thick	l	po	wbm
G61	**Ul**	p	thick	p	thick	c,l,o	po	wbm
G61	**Ca**	p	thick	p	thick	l,o	po	wbm
G61	**Fe**	p	thin	p	thick	c,l,o	po	wbm
G61	**Ti**	p	thin	p	thin	l	po,few so,few rc	wbm
G61	**Ta**	p	thin	p	thin	l,o	po	wbm
G24	**Hu**	p	thin	p	thick	c,l,o	po	wbm, few lb
G24	**Ra**	p	thick	p	thick	l	po	wbm
G24	**Ul**	p	thin	p	thick	o	po	wbm
G24	**Ca**	p	thin	p	thick	c,l,o	po	wbm, few lb
G24	**Fe**	p	thick	p	thick	c,o	po	wbm, few lb
G24	**Ti**	p	thin	p	thick	l,o	po	wbm
G24	**Ta**	p	thin	p	thick	l	po	wbm
G56	**Hu**	p	thin	p	thick	c,l,o	po,few so	wbm, few lb
G56	**Ra**	p	thin	p	thick	l	po,few rc	wbm
G56	**Ul**	p	thin	p	thick	c,l	po	wbm
G56	**Ca**	p	thin	p	thick	l	po	wbm
G56	**Fe**	p	thin	p	thick	c,l,o	po	wbm, few lb
G56	**Ti**	p	thin	p	thick	o	po	wbm
G56	**Ta**	p	thin	p	thin	l,o	po,few so,few rc	wbm, few lb
G57	**Hu**	p	thin	p	thick	c,o	po	wbm
G57	**Ra**	p	thin	p	thick	l,o	po	wbm
G57	**Ul**	p	thin	p	thin	c,l,o	po	wbm
G57	**Ca**	p	thin	p	thick	l	po	wbm
G57	**Fe**	p	thin	p	thin	c,o	po	wbm
G57	**Ti**	p	thin	p	thick	l	po	wbm
G57	**Ta**	p	thick	p	thick	l,o	po,few so	wbm

Table A8: Descriptive statistics for the *k* index averages for the different bones of African penguin specimens. CI: Confidence interval at 95%.

Type of bone	Age	AFRICAN PENGUIN				CAPE GANNET			
		Mean	Standard deviation	Lower CI	Upper CI	Mean	Standard deviation	Lower CI	Upper CI
HUMERUS	**Juvenile**	0.13	0.10	0.01	0.38	0.75	0.03	0.70	0.79
	Adult	0.22	0.09	0.13	0.31	0.73	0.03	0.69	0.77
RADIUS	**Juvenile**	0.18	0.16	0.01	0.57	0.74	0.01	0.71	0.76
	Adult	0.25	0.10	0.15	0.35	0.72	0.03	0.67	0.76
ULNA	**Juvenile**	0.12	0.15	0.01	0.49	0.78	0.03	0.73	0.82
	Adult	0.19	0.13	0.06	0.32	0.77	0.04	0.72	0.81
CARPOMETACARPUS	**Juvenile**	0.25	0.15	0.02	0.63	0.76	0.03	0.71	0.81
	Adult	0.28	0.15	0.09	0.46	0.74	0.04	0.69	0.79
FEMUR	**Juvenile**	0.36	0.05	0.24	0.49	0.77	0.02	0.74	0.79
	Adult	0.43	0.03	0.36	0.50	0.78	0.03	0.75	0.82
TIBIOTARSUS	**Juvenile**	0.33	0.08	0.13	0.53	0.72	0.01	0.70	0.73
	Adult	0.46	0.05	0.41	0.52	0.76	0.02	0.73	0.78
TARSOMETATARSUS	**Juvenile**	0.29	0.08	0.10	0.48	0.72	0.05	0.64	0.79
	Adult	0.40	0.18	0.21	0.59	0.72	0.05	0.66	0.78

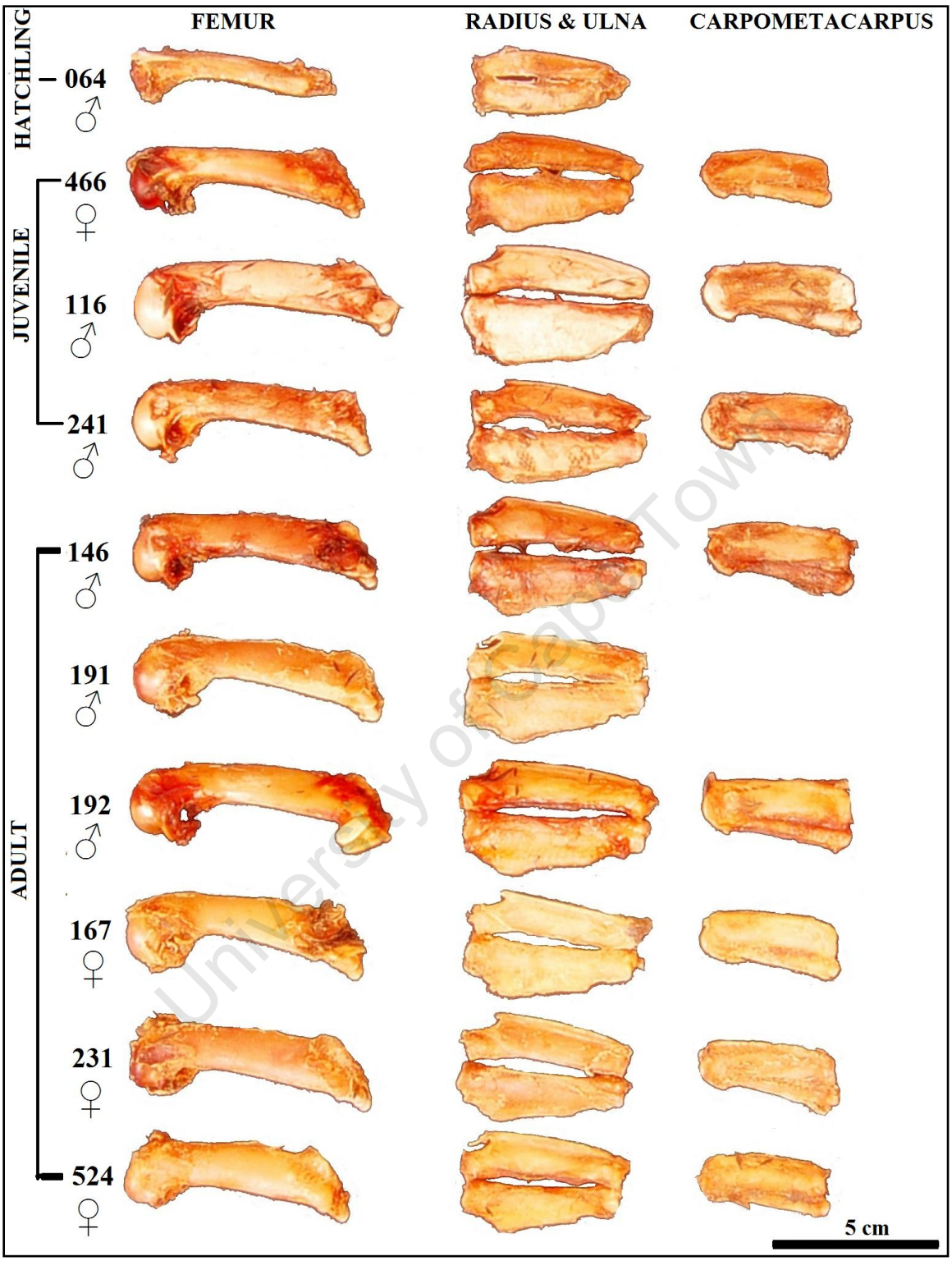

Figure A1: Fore-limb bones of the African Penguin (*Spheniscus demersus*) sampled for histological study. The bones are presented with their proximal side on the left. The specimens are arranged based on their ontogenetic stage and gender (male ♂, female ♀). (Scale bar: 5cm).

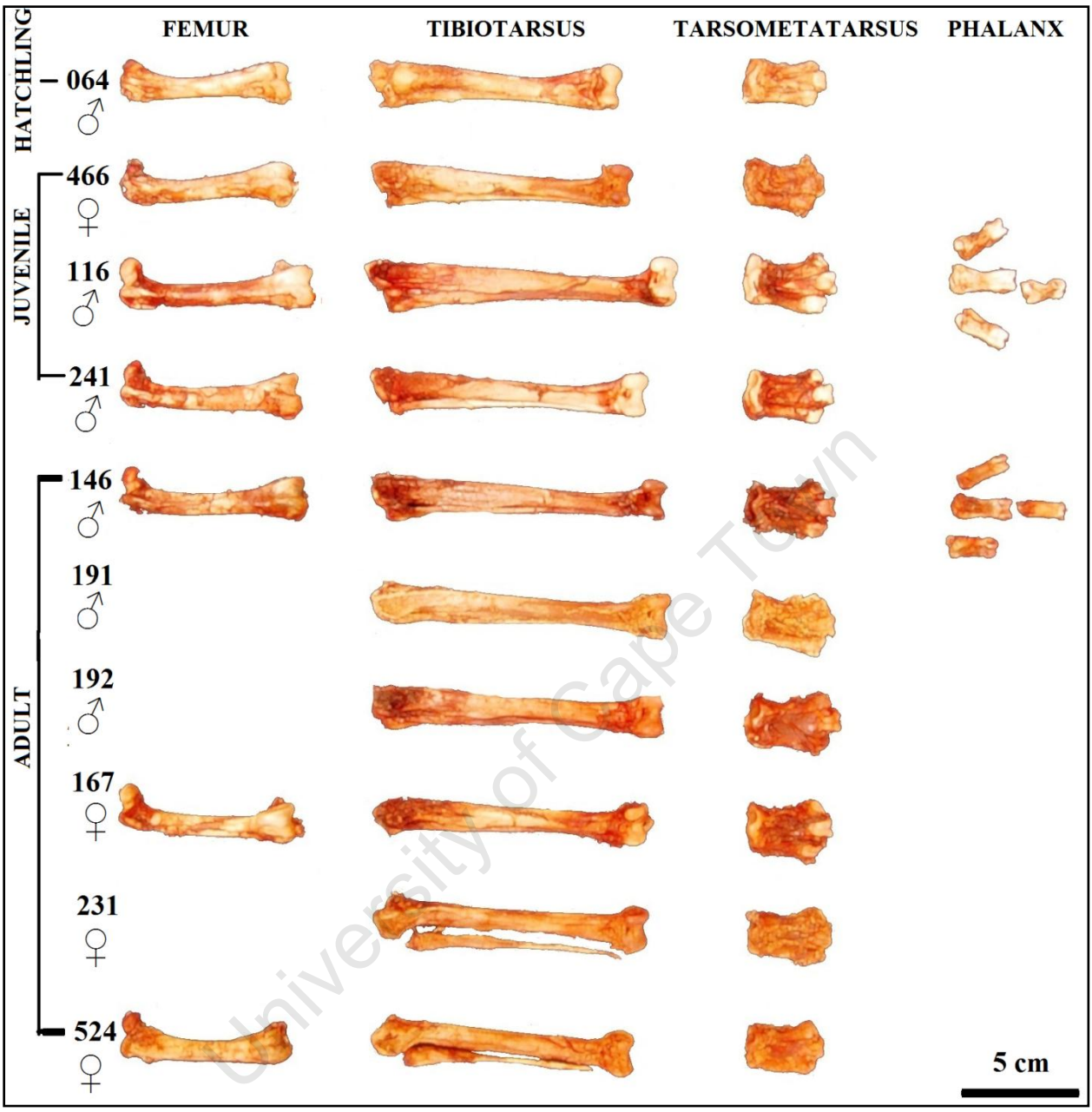

Figure A2: Hind limb bones of the African Penguin (*Spheniscus demersus*) sampled for histological study. The bones are presented with their proximal side on the left. The specimens are arranged based on their ontogenetic stage and gender (male ♂, female ♀). (Scale bar: 5cm).

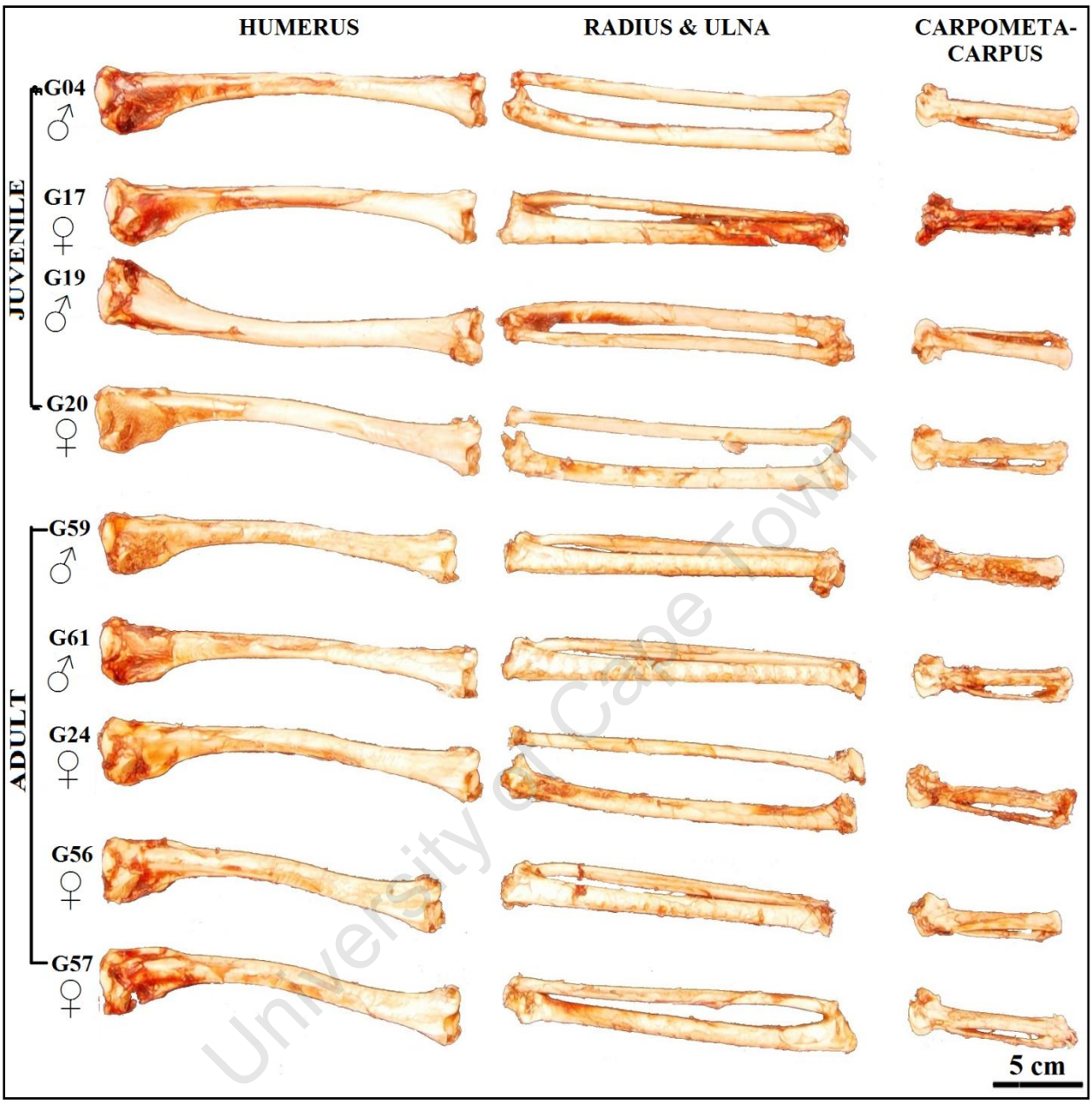

Figure A3: Fore-limb bones of the Cape gannet (*Morus capensis*) sampled for histological study. The bones are presented with their proximal side on the left. The specimens are arranged based on their ontogenetic stage and gender (male ♂, female ♀). (Scale bar: 5cm).

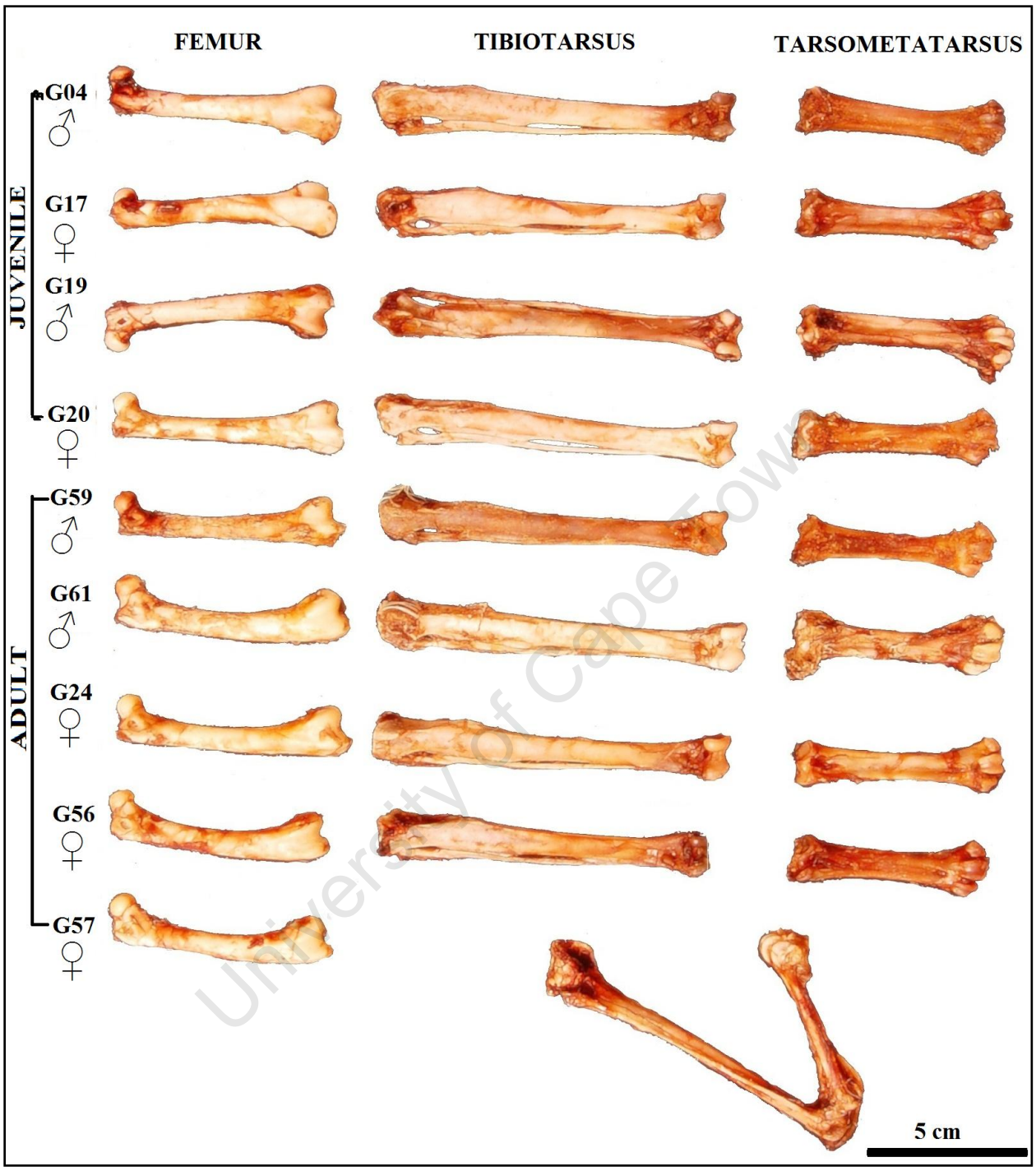

Figure A4: Hind limb bones of the Cape gannet (*Morus capensis*) sampled for histological study. The bones are presented with their proximal side on the left. The specimens are arranged based on their ontogenetic stage and gender (male ♂, female ♀). (Scale bar: 5cm).